MOLECULAR AND CELLULAR BIOLOGY, Feb. 2002, p. 816–834 Vol. 22, No. 3
0270-7306/02/$04.00+0 DOI: 10.1128/MCB.22.3.816–834.2002
Copyright © 2002, American Society for Microbiology. All Rights Reserved.

Hsp27 as a Negative Regulator of Cytochrome *c* Release

Catherine Paul, Florence Manero, Sandrine Gonin, Carole Kretz-Remy, Sophie Virot, and André-Patrick Arrigo*

Centre de Génétique Moléculaire et Cellulaire, CNRS-UMR-5534, Université Claude Bernard Lyon I, F-69622 Villeurbanne, France

Received 12 March 2001/Returned for modification 18 April 2001/Accepted 29 October 2001

We previously showed that Hsp27 protects against apoptosis through its interaction with cytosolic cytochrome *c*. We have revisited this protective activity in murine cell lines expressing different levels of Hsp27. We report that Hsp27 also interferes, in a manner dependent on level of expression, with the release of cytochrome *c* from mitochondria. Moreover, a decreased level of endogenous Hsp27, which sensitized HeLa cells to apoptosis, reduced the delay required for cytochrome *c* release and procaspase 3 activation. The molecular mechanism regulating this function of Hsp27 is unknown. In our cell systems, Hsp27 is mainly cytosolic and only a small fraction of this protein colocalized with mitochondria. Moreover, we show that only a very small fraction of cytochrome *c* interacts with Hsp27, hence excluding a role of this interaction in the retention of cytochrome *c* in mitochondria. We also report that Bid intracellular relocalization was altered by changes in Hsp27 level of expression, suggesting that Hsp27 interferes with apoptotic signals upstream of mitochondria. We therefore investigated if the ability of Hsp27 to act as an expression-dependent modulator of F-actin microfilaments integrity was linked to the retention of cytochrome *c* in mitochondria. We show here that the F-actin depolymerizing agent cytochalasin D rapidly induced the release of cytochrome *c* from mitochondria and caspase activation. This phenomenon was delayed in cells pretreated with the F-actin stabilizer phalloidin and in cells expressing a high level of Hsp27. This suggests the existence of an apoptotic signaling pathway linking cytoskeleton damages to mitochondria. This pathway, which induces Bid intracellular redistribution, is negatively regulated by the ability of Hsp27 to protect F-actin network integrity. However, this upstream pathway is probably not the only one to be regulated by Hsp27 since, in staurosporine-treated cells, phalloidin only partially inhibited cytochrome *c* release and caspase activation. Moreover, in etoposide-treated cells, Hsp27 still delayed the release of cytochrome *c* from mitochondria and Bid intracellular redistribution in conditions where F-actin was not altered.

The molecular mechanisms leading to apoptosis require the activation of cysteine proteases, referred to as caspases (54), which are synthesized as inactive precursors, procaspases, and activated by proteolytic cleavage (73). Mitochondria as well as several mitochondrial proteins play a central role in the activation of procaspases (18, 61). In mammalian cells committed to apoptosis, mitochondrial proteins, such as cytochrome *c*, AIF (apoptosis inducing factor), Hsp60, Hsp10, adenylate kinase, and smac/diablo as well as procaspases 2, 3, 8, and 9, are released in the cytosol (13, 31, 32, 65, 69, 70, 77, 80, 82). Interaction of cytochrome *c* with Apaf-1 in the presence of ATP/dATP results in the formation of the apoptosome complex, which contains and activates procaspase 9, which in turn activates procaspase 3 (40). The translocation of cytochrome *c* from mitochondria to cytosol occurs very early during the apoptotic process, usually before mitochondrial membrane potential loss and independently of caspase activity (7, 17, 84). This phenomenon may be induced by conformational changes of Bax that are triggered by CIF/Bid (11, 22, 44, 79).

Several cellular antiapoptotic proteins have been described which include members of the Bcl-2 (6, 76) and IAP (inhibitor of apoptosis proteins) (12) families, Hsp70 (29, 38, 53, 66), Hsp90 (56), and Hsp27 (2, 9, 14, 50, 55, 66, 72, 78). Bcl-2 regulates the release of apoptogenic cytochrome *c*, probably by interfering with the mitochondrial channel VDAC (68), and also acts more downstream by inhibiting caspase activation (63). IAP interferes with caspase activity (12), while Hsp70 interacts with BAG-1 (71) and inhibits apoptosis by preventing recruitment of procaspase 9 to the Apaf-1 apoptosome complex (3). Hsp70 has also been reported to act downstream of caspase activation (29), while Hsp90 appears to inhibit apoptosome formation (56). Expression of these proteins in tumor cells usually suppresses apoptosis induced by a wide range of stimuli, leading to aggressively growing and chemoresistant tumors. In this respect, it has been shown that overexpression of Hsp70 (28) increases the tumorigenicity of different transformed cells. In the case of Hsp27, the physiological significance of Hsp27 overexpression has been clearly demonstrated in our recent reports showing that the overexpression of this protein enhanced the tumorigenic potential of rat colon carcinoma cells (REG cells) when they were reimplanted in syngeneic rats (10, 15). This effect correlated with reduced in vivo apoptosis of the tumor cells.

Mammalian small stress proteins (sHsp), including αAB-crystallins and the major Hsp27 polypeptide, are oligomeric phosphoproteins that belong to the superfamily of heat shock or stress proteins (Hsp) (2). In vitro, Hsp27 displays an ATP-independent chaperone activity (30) that requires a high degree of Hsp27 oligomerization to be active (62). Monomeric and nonphosphorylated Hsp27 has also been described as a

* Corresponding author. Mailing address: Centre de Génétique Moléculaire et Cellulaire, CNRS-UMR-5534, Université Claude Bernard Lyon I, 16 rue Dubois, Bat. Gregor Mendel, F-69622 Villeurbanne, France. Phone: 33 (0) 472448595. Fax: 33 (0) 472440555. E-mail: arrigo@univ-lyon1.fr.

potent in vitro modulator of actin polymerization. Hsp27 is thought to cap the barbed end of the actin filament, thus inhibiting the addition of monomers and subsequently filament growth (4, 52). In vivo, expression of Hsp27 increases cellular resistance against heat shock (1) and different other injuries, such as those mediated by chemotherapeutic drugs (2) or oxidative stress (e.g., tumor necrosis factor alpha) (46, 62). This protection may be a result of the reduced-glutathione-dependent in vivo chaperone activity of Hsp27 against misfolded or oxidized proteins (59) and/or of the stabilization of actin microfilaments by Hsp27 (19, 27, 34, 36, 43). Hsp27 has also been indirectly implicated in membrane blebbing formation by stressing agents through its SAP kinase 2-triggered actin polymerization-generating activity (26).

Hsp27 can also modulate apoptosis induced independently of reactive oxygen species production. In this respect, we and others have reported that Hsp27 exerts an antiapoptotic effect in cells exposed to staurosporine, Fas/APO-1 (2, 50), actinomycin D, camptothecin, etoposide (66), cisplatin (16), and doxorubicin (23). We also showed that the transient expression of Hsp27 during early differentiation could counteract the apoptotic process inherent to cell differentiation (45, 47). In contrast, Hsp27 protects less efficiently against T-antigen- or p53-mediated cell death (20) and has been reported to promote apoptosis mediated by cytotoxic T-lymphocyte cells (5). Recently, we reported that human Hsp27 reduces apoptosis by counteracting procaspase 9 activation without altering cytochrome *c* release (14). This inhibition of procaspase 9 activation is probably a consequence of the binding of Hsp27 to cytosolic cytochrome *c*, a phenomenon that subsequently down-regulates apoptosome formation (9). The binding of Hsp27 to caspase 3 and its probable modulation by this stress protein have been documented (55). We also recently reported that Hsp27 expression did not counteract granzyme B-mediated activation of procaspases, indicating that this stress protein probably does not act downstream of caspase-3 (9).

Here, we have performed a new analysis of the protective activity of Hsp27 against apoptosis using different cell lines that overexpress or underexpress Hsp27. We report that, in cells exposed to staurosporine, etoposide, or cytochalasin D, Hsp27 interferes, in a manner dependent on level of expression, with the release of cytochrome *c* in the cytosol. This activity requires a higher level of Hsp27 expression compared to the activity that interferes with procaspase activation downstream of cytochrome *c* release. The retention of cytochrome *c* in the mitochondria of cells overexpressing Hsp27 was correlated with an alteration of Bid intracellular redistribution. At least in cytochalasin D-treated cells, the protective activity of Hsp27 against F-actin destruction may play a role in the interference mediated by this stress protein against Bid intracellular redistribution and the release of cytochrome *c* in the cytosol.

MATERIALS AND METHODS

Cell lines. Small Hsp-expressing murine fibrosarcoma L929 cell lines (L929-Hsp27; human Hsp27 and L929-Hsp25; murine Hsp27) were, respectively, derived from previously characterized L929-27-3 and L929-Wt-25 cells (48, 58). L929-Hsp27 cells express 0.9 ng of human Hsp27 per μg of total proteins while L929-Hsp25 cells express 0.45 ng of murine Hsp27 per μg. L929 cells expressing 0.15 ng (L929-Hsp25wt-1 cells) or 0.10 ng (L929-Hsp25wt-2 cells) of murine Hsp27 per μg were also analyzed. L929-Hsp25wt-1 cells were derived from previously characterized L929-Wt-16 cells (60). The level of expression of either human Hsp27 or murine Hsp27 was estimated in immunoblots that also contained serial dilutions of the corresponding purified protein. Control cell lines (L929-C2 and -C3) were isolated after cotransfection of the hygromycin resistance-bearing plasmid with the pSVK3 plain vector. Murine NIH 3T3 fibroblasts expressing human Hsp27 were obtained by exposing cells (2×10^6 cells/78-cm^2 Falcon dish) to calcium phosphate DNA precipitates containing 15 μg of the human Hsp27 expression vector KS2711ΔHK (46) and 1 μg of pMC1 neopolyA plasmid carrying the neomycin resistance gene. At 24 h after removal of DNA precipitates, G418 (500 μg/ml; Sigma, St. Louis, Mo.) was added to the culture medium. After 3 weeks of selection with G418, resistant single-cell clones were isolated and characterized. HeLa cells underexpressing Hsp27 were isolated after transfection with a pCIneohsp27 antisense vector. This vector contains the entire coding sequence of the hsp27 gene placed in reverse orientation under the control of the cytomegalovirus promoter and neomycin gene selection. pCIneohsp27 antisense was constructed using an *Eco*RI-*Eco*RI DNA fragment of plasmid psvhsp27 (48), which was inserted in the *Eco*RI site of pCIneo vector (Promega, Charbonnieres, France). HeLa cells (2.1×10^6) were transfected according to the Fugene 6 procedure (Roche Diagnostics, Meylan, France) using 6.8 μg of pCIneohsp27 antisense vector or the void pCIneo vector. After 3 weeks of selection with G418 (500 μg/ml), resistant single-cell clones were isolated and characterized. All these cells were grown at 37°C in Dulbecco's modified Eagle medium containing 10% fetal calf serum.

Reagents. Anti-murine Hsp27, anti-Hsc70 (clone C92), and anti-human Hsp27 antibodies were purchased from Stressgen (Victoria, British Columbia, Canada). Anti-cytochrome *c* (clone 7H8.2C12 for immunoblotting and clone 6H2.B4 for immunofluorescence analysis) and anti-caspase 3 antibodies were from Pharmingen (San Diego, Calif.). Anti-cytochrome oxidase (subunit II) (Cox) antibody (clone 12C4.F12) and Alexa Fluor 488 phalloidin were from Molecular Probes/Interchim (Montlucon, France). Anti-Bcl-2 and anti-Bid antibodies were from Santa Cruz Biotechnology-Tebu (Le Perray en Yvelines, France). We also used antibodies against human Hsp27 and ATP synthase F1 complex that were kindly provided to us by R. M. Tanguay (Laval University, Ste. Foy, Canada) and C. Godinot (CNRS 5534, Lyon, France), respectively. z-VAD-fmk was from R&D systems (Abingdon, United Kingdom). Crystal violet, staurosporine, cytochalasin D, phalloidin, etoposide, and L-buthionine-(*S*,*R*)-sulfoximine (BSO) were purchased from Sigma.

Assessment of resistance to cell death. Crystal violet staining of the cells was used to analyze the resistance of cells to death. In this case, cells (10^4/well) were grown in 96-well plates for 24 h before being analyzed. Following incubation with apoptosis-inducing agents, the remaining viable cells were stained with 0.5% crystal violet in 20% methanol for 15 min. Microtiter plates were rinsed and dried. A solution containing 0.1 M sodium citrate, pH 4.2, and 50% methanol was then added to solubilize the stained cells. The absorbance of each well was read at 550 nm with an MR500 MicroElisa reader (Dynatech Laboratories, Chantilly, France). Percent viability was defined as the relative absorbance of treated versus untreated control cells.

Cytochrome *c* release from mitochondria. The method described by Bossy-Wetzel et al. (7) was used with some modifications. In brief, about 2×10^6 cells were harvested and subsequently washed twice in ice-cold phosphate-buffered saline (PBS), pH 7.4. The cells were then spun at $200 \times g$ for 5 min. The cell pellet was resuspended in 600 μl of extraction buffer containing 220 mM mannitol, 250 mM sucrose, 50 mM PIPES-KOH (pH 7.4), 50 mM KCl, 5 mM EGTA, 2 mM $MgCl_2$, 1 mM dithiothreitol, and protease inhibitors (complete cocktail from Boehringer Mannheim/Roche Diagnostics, Meylan, France). After a 30-min incubation on ice, cells were homogenized with a glass Dounce homogenizer and a B pestle (80 strokes) and spun for 15 min at $14{,}000 \times g$. Pellets were directly resuspended in sodium dodecyl sulfate (SDS) Laemmli sample buffer while supernatants were then diluted 1:1 in 2× SDS Laemmli sample buffer before being boiled for 5 min. Analysis was performed in SDS–16.5% polyacrylamide gels. Gels were then processed for immunoblotting as described below.

Measurement of caspase activity. For the in vivo determination of DEVD-dependent procaspase 3-like activation, cells (10^6) were harvested and subsequently washed twice in ice-cold PBS, pH 7.4. They were then spun at $200 \times g$ for 5 min, and the dry cell pellets were stored at −80°C. The determination of DEVD-AFC activity was performed using the Apo Alert CPP32 fluorometric assay kit (Clontech, Montigny les Bretonneux, France). For procaspase 8, IETD-AFC activity was determined using the same protocol and the Apo Alert FLICE fluorometric assay kit (Clontech). Excitation was at 400 nm and emission was at 505 nm in a Victor Wallach cytofluorometer (EG&G Instruments, Evry, France).

Cellular fractionation. Cells were fractionated according to the method of Trounce et al. (74). Cells (6×10^6) were harvested in cold PBS, and the cell pellet weight was recorded. Cells were then resuspended and incubated for 10 min in ice-cold hypotonic buffer A (20 mM HEPES-KOH, pH 7.4; 1 mM EGTA)

at a ratio of 4 ml per g of packed cells. An equal volume of buffer A supplemented with 0.5 M mannitol was then added to the cell suspension to render the medium isotonic. The suspension was then transferred to a chilled glass Dounce homogenizer. Thirty to fifty passes of a Teflon pestle were necessary to disrupt all cells. Following centrifugation at 600 × *g* for 2 min (Pellet-0.6 and Sup-0.6), the resulting supernatant (Sup-0.6) was then spun at 700 × *g* for 10 min [Pellet-0.7(1) and Sup-0.7(1)] and this step was repeated once [Pellet-0.7(2) and Sup-0.7(2)]. The remaining supernatant Sup-0.7(2) was subsequently spun at 10,000 × *g* for 20 min [Pellet-10(1) and Supernatant-10(1)]. Pellet-10(1) was resuspended in isotonic buffer A and spun again for 20 min at 10,000 × *g* [Pellet-10(2) and Supernatant-10(2)]. The Pellet-10(2) is enriched in mitochondria. Collected fractions were then analyzed in immunoblots and tested for the presence of human or murine Hsp27, Bcl-2 and mitochondrial markers such as the β-subunit of the ATP synthase F1 complex and cytochrome *c*. For the analysis of the presence of Bid in the cytosol, 4×10^6 cells were lysed in a buffer containing 10 mM Tris HCl (pH 7.4), 1 mM $MgCl_2$, 0.1 mM EDTA, and 10 mM NaCl and spun for 10 min at 2,000 × *g* (Pellet 2000 × *g* [P2]). The resulting supernatant was further spun for 10 min at 20,000 × *g* (P20 and S).

Immunoblotting and gel electrophoresis. Immunoblots and gel electrophoresis were done as already described (59). The detection of the immunoblots was performed with the ECL kit from Amersham Corp. (United Kingdom). Autoradiographs were recorded onto X-Omat LS films (Eastman Kodak Co., Rochester, N.Y.) and scanned with the Bioprofil system (Vilber Lourmat, Marne-la-Vallée, France). The duration of the exposure was calculated to be in the linear response of the film.

Immunofluorescence analysis. Cells were plated at a density of 2×10^4 cells/cm^2 on glass slides and were allowed to attach for 18 h. Cells were either kept untreated or treated with various concentrations of staurosporine, cytochalasin D, or etoposide. To observe F-actin architecture, cells were fixed for 10 min with fresh 3.7% formaldehyde in PBS and subsequently permeabilized 5 min in cold acetone. F-actin was stained for 20 min with Alexa Fluor 488 phalloidin (5 U per ml of PBS). Cells were then observed under a Zeiss Axioskop microscope equipped with a 63× objective lens with a 1.25 numerical aperture and recorded onto Illford XP2 super films.

Confocal microscopy. L929-Hsp27 or HeLa cells (7×10^5) were seeded in 60-mm-diameter dishes containing coverslips (18 mm in diameter) 1 day before being analyzed. To compare Hsp27 and Cox localization, fixation was performed by exposing cells for 90 s to methanol maintained at −20°C. Cells were stained by incubating the coverslips for 1 h with anti-Hsp27 (diluted 1/100 in PBS containing 0.1% bovine serum albumin [BSA]) and anti-Cox (10 μg/ml in PBS containing 0.1% BSA) antibodies. After washing, Hsp27 and Cox staining was revealed by incubating cells for 1 h with fluorescein isothiocyanate (FITC)-conjugated goat anti-rabbit immunoglobulin G (IgG) and tetramethyl rhodamine isothiocyanate (TRITC)-conjugated goat anti-mouse IgG (1/200 in PBS containing 0.1% BSA), respectively. Control experiments performed with nonimmune sera or with only the second antiserum confirmed that all detectable fluorescence was specific. Experiments aimed at analyzing cytochrome *c* were performed by fixing the cells for 10 min with 3.7% formaldehyde, pH 7.4, in PBS. Permeabilization was for 3.5 min in 0.2% Triton X-100. Cells were stained for 2 h with anti-native cytochrome *c* antibody (diluted 1/15 in PBS containing 0.1% BSA). After washing, cytochrome *c* staining was revealed by incubating cells for 2 h with TRITC-conjugated goat anti-mouse IgG (1/200 in PBS containing 0.1% BSA). Examination of samples was performed in an LSM510 laser scanning confocal microscope (Zeiss) using a 63× (numerical aperture, 1.4) Zeiss Plan Neo Fluor objective. Illumination sources were 488 nm and 543 nm. To avoid cross talk between the different fluorochromes, the multitrack recording module was used, which allows a sequential acquisition of each channel.

RESULTS

Characterization of Hsp27-expressing cell lines. Immunoblot analysis of either human Hsp27 (hHsp27) or murine Hsp27 (mHsp27) expression in transfected L929 cell clones is presented in Fig. 1A. A comparison with the signals generated by serial dilutions of the corresponding pure protein revealed that L929-Hsp27 cells contain 0.9 ng of human Hsp27 per μg of total cellular proteins while 0.45 and 0.15 ng of murine Hsp27 are expressed per μg of total proteins in L929-Hsp25 and L929-Hsp25wt-1 cells, respectively. Another L929 cell line (L929-Hsp25wt2) that expresses murine Hsp27 at 0.1 ng/μg was also analyzed. Control L929-C2 and L929-C3 (not shown) cells are devoid of Hsp27 expression. Apoptotic inducers such as staurosporine or etoposide were not found to induce or modify the level of Hsp27 expression (not shown). As already described (14, 50), Hsp27 induces a cellular protection against staurosporine or etoposide which is related to its level of expression (not shown).

Analysis of the proteolytic activity associated with caspase activation revealed that the fluorogenic polypeptide DEVD-AFC started to be cleaved by caspase 3-like proteases when L929-C2 (Fig. 1B) or L929-C3 (not shown) cells were treated for at least 2 h with 1 μM staurosporine. A 3.5-fold increase in caspase activation was then observed after 8 h of treatment. In contrast, the expression of 0.9 ng of human Hsp27 per μg completely inhibited the cleavage of DEVD-AFC that is normally observed during the first 4 h of staurosporine treatment. A 6-h treatment was necessary to detect a weak cleavage activity in the cytosolic extracts of Hsp27-expressing cells. By 8 h, this activation represented less than 20% of that normally observed in control cells. Expression of murine Hsp27 (0.45 ng/μg) also decreased the activation of DEVD-dependent caspases. This decreased activation was, however, not as intense as that observed in cells expressing human Hsp27. The comparison of the effect induced by murine Hsp27 in L929-Hsp25 cells with those induced in L929-Hsp25wt1 (Fig. 1B) and -Hsp25wt2 (data not shown) cells revealed that the protection against procaspase 3-like activation was dependent on the level of murine Hsp27 expression. Similar results were observed when these different cells were exposed to etoposide (data not shown).

Analysis of procaspase 8 activity (Fig. 1, insert) revealed that its activation by staurosporine treatment occurred at a later time than that of DEVD-dependent caspases. Indeed, in control L929 cells, procaspase 8 activation was detectable only after 6 h of staurosporine treatment. After 3 h of treatment, the activation index of this caspase was even lower than that observed in untreated cells. The reason for this reproducible decrease is unknown. In L929-Hsp27 cells, no activation was detected during the first 6 h of treatment. This suggests that in our cell system the activation of procaspase 8 occurs downstream of procaspase 3 activation by cytochrome *c*.

Interference of Hsp27 level of expression with cytochrome *c* release from mitochondria in murine cells exposed to staurosporine. We next determined whether Hsp27 interfered with cytochrome *c* release from mitochondria since this phenomenon is a critical step that occurs upstream of caspase activation in murine fibroblasts treated with staurosporine (7). This was assessed by monitoring the presence of cytochrome *c* in the soluble cytoplasm at various times, before and after adding 1 μM staurosporine to the cell medium. L929 cells were harvested and lysed under conditions that kept mitochondria intact, and the lysate was then spun at 14,000 × *g* to obtain a supernatant and a mitochondrion-containing pellet fraction as described in Materials and Methods. It is seen in the immunoblots presented in Fig. 2A that cytochrome *c* was not detectable in the supernatant fraction of untreated control L929-C2 cells. This protein was quantitatively recovered in the mitochondrion-containing 14,000 × *g* pellet fraction. Following cell exposure to staurosporine, cytochrome *c* was detectable in the soluble fraction already after 1 h of treatment and

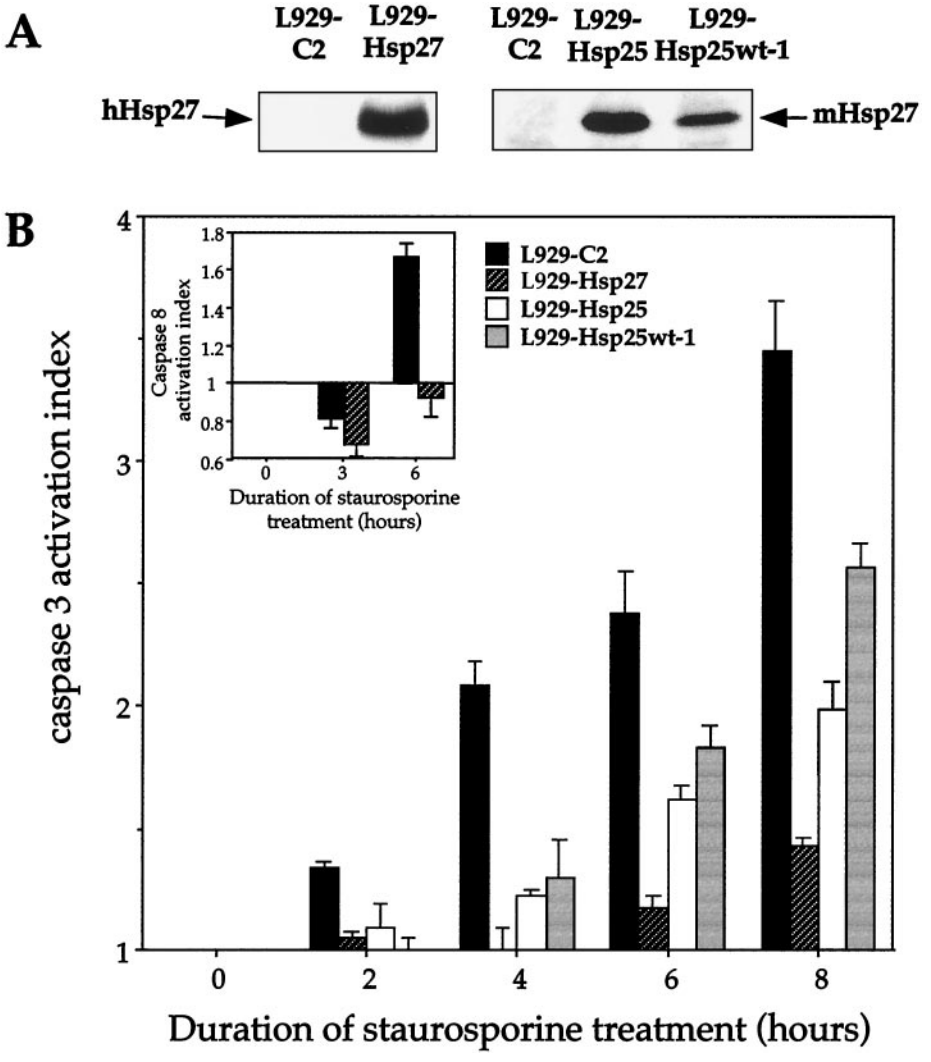

FIG. 1. Characterization of staurosporine-resistant L929 cells expressing Hsp27. (A) Characterization of human Hsp27 (hHsp27) levels in L929-Hsp27 cells and murine Hsp27 (mHsp27) levels in L929-Hsp25 and L929-Hsp25wt-1 cells. Total cellular proteins were analyzed in immunoblots probed with antisera that recognized either hHsp27 or mHsp27 as outlined in Materials and Methods. L929-C2, control cells. (B) Activity of DEVD-specific caspases measured using the fluorescent substrate DEVD-AFC as described in Materials and Methods. The activation index was determined as the ratio between the activity in extracts of treated cells to that measured in extracts of nontreated cells. The histogram shown is representative of three identical experiments; standard deviations (error bars) are presented ($n = 3$). The insert shows caspase 8 activity measured using the fluorescent substrate IETD-AFC.

was maximally released after 2 h of treatment. The absence of cytochrome oxidase (subunit II; Cox) in the soluble fractions indicated that mitochondrial integrity was preserved. Similar observations were made when control L929-C3 cells were analyzed (not shown). When the same type of analysis was performed with cells expressing 0.9 ng of human Hsp27 per μg of total cellular proteins, cytochrome *c* was barely detectable in the supernatant fraction during the first 12 h (the first 6 h are shown in Fig. 2A) of staurosporine treatment.

We next analyzed whether the lack of detection of cytochrome *c* in the cytosol of L929-Hsp27 cells treated with staurosporine was due to a retention of this apoptogenic agent in the mitochondrion-containing pellet resulting from centrifugation at 14,000 × *g* or to a degradation of this protein. This was performed by analyzing the level of cytochrome *c* present in mitochondrion-containing pellets isolated from untreated and staurosporine-treated L929-C2 and L929-Hsp27 cells. As seen in Fig. 2B, staurosporine treatment induced a sharp decline in the level of cytochrome *c* present in the pellet fraction isolated from control cells. In contrast, the level of cytochrome *c* present in the pellet isolated from L929-Hsp27 cells remained constant. Hence, in cells expressing human Hsp27 at 0.9 ng/μg, cytochrome *c* remains associated with the mitochondrion-containing pellet resulting from centrifugation at 14,000 × *g* and is not degraded.

We next analyzed the behavior of cytochrome *c* in the other cell lines which expressed different levels of murine Hsp27. It is seen in Fig. 3 that the expression of murine Hsp27 (L929-Hsp25 cells) at 0.45 ng/μg interfered with the appearance of cytochrome *c* in the cytosolic fraction of staurosporine-treated

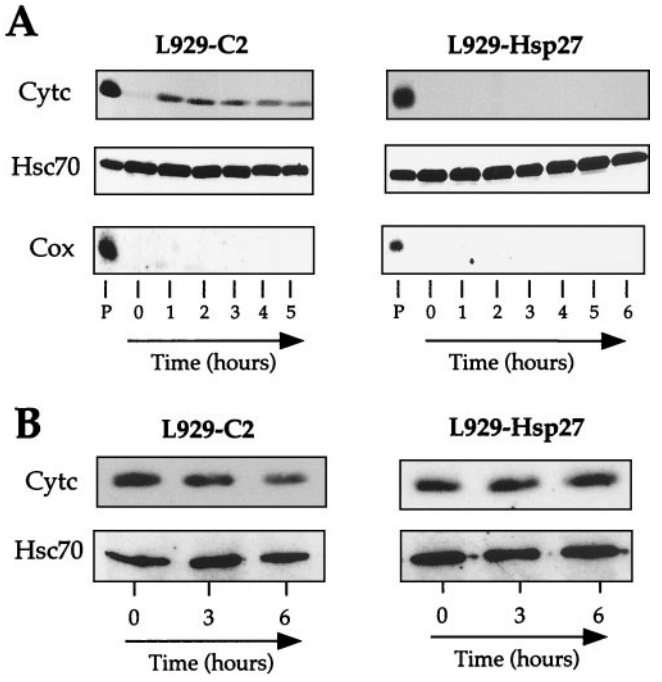

FIG. 2. Human Hsp27 expression interferes with the accumulation of cytosolic cytochrome *c* in response to staurosporine treatment. Control (L929-C2) and human Hsp27-expressing (L929-Hsp27) cells were either kept untreated or treated for various times with 1 μM staurosporine. Cells were then harvested, lysed under conditions that kept mitochondria intact, and spun to obtain a supernatant (A) and a pellet fraction resulting from centrifugation at 14,000 × *g* (B) as described in Materials and Methods. The presence of cytochrome *c* (Cytc), Hsc70, and cytochrome oxidase (subunit II) (Cox) in the different fractions was determined by immunoblot analysis. Hsc70 was used as an internal marker of gel loading. Autoradiographs of ECL-revealed immunoblot are presented. Note that in human Hsp27-expressing cells, cytochrome *c* is not detectable in the supernatant and most of this protein remains associated with the pellet fraction. Lanes: P, pellet from untreated cells; 0 to 6, soluble fractions isolated from either untreated cells (0) or cells treated for the indicated number of hours with staurosporine.

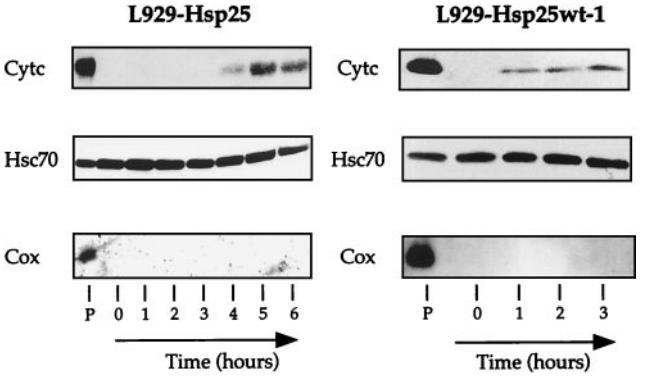

FIG. 3. Analysis of L929 cells expressing different levels of murine Hsp27. The interference with the accumulation of cytosolic cytochrome *c* depends on Hsp27 level. Murine Hsp27-expressing L929-Hsp25 and L929-Hsp25wt-1 cells were either kept untreated or treated for various times with 1 μM staurosporine. Cells were processed, and the presence of cytochrome *c*, Hsc70, and Cox was determined as described in the legend to Fig. 2. Only the immunoblot analysis of the supernatant fractions (1 to 6) and pellet fraction (P) isolated at time zero are presented. Note that the interference of Hsp27 with cytochrome *c* release is dependent on the level of expression of this stress protein.

L929 cells. The interference was, however, less intense than the one observed in the case of human Hsp27 since, in L929-Hsp25 cells, cytochrome *c* started to be efficiently detected in the soluble fraction after 4 to 5 h of treatment with 1 μM staurosporine. Analysis of the level of cytochrome *c* that remained in the pellet fraction confirmed that, similarly to human Hsp27, murine Hsp27 delayed the appearance of cytochrome *c* in the soluble cytoplasmic fraction (not shown).

The analysis of L929-Hsp25wt-1 cells, which contain about three times less murine Hsp27 than L929-Hsp25 cells, revealed that cytochrome *c* was already detectable in the soluble fraction after 1 h of treatment, observed in control cells (Fig. 2A and 3). Similar results were obtained when L929-Hsp25wt-2 cells, which express murine Hsp27 at 0.10 ng/μg, were analyzed (not shown). Hence, an expression of murine Hsp27 at 0.10 to 0.15 ng/μg did not significantly alter the detection of cytochrome *c* in the soluble fraction of L929 cells exposed to staurosporine. However, as seen in Fig. 1, this small level of murine Hsp27 expression still induced some protection against caspase 3 activation. This confirms earlier studies showing that low levels of Hsp27 expression can interfere with caspase activation independently of any effect on cytochrome *c* (15, 55).

The Hsp27-mediated retention of cytochrome *c* in the pellet resulting from centrifugation at 14,000 × *g* is not specific to staurosporine treatment or L929 cells and is also not glutathione dependent. We investigated whether human Hsp27 or murine Hsp27 was also effective at counteracting the detection of soluble cytochrome *c* when apoptosis was induced by etoposide. It is seen in Fig. 4A that, similarly to staurosporine, etoposide (500 μM) induced a rapid accumulation of cytochrome *c* in the cytosol of control L929-C2 cells. In contrast, both human and murine Hsp27 expression inhibited this phenomenon, at least during the first 4 h of the treatment (Fig. 4B and C). Similar observations were made when cells were treated with cytochalasin D (0.5 μM) (see Fig. 11A). Similar observations were made when cells were exposed to a heat shock treatment (not shown), confirming our preceding results obtained in Jurkat cells (67).

We have reported that, in L929 and NIH 3T3-ras cells, the protective activity mediated by Hsp27 against tumor necrosis factor alpha and oxidative stress is glutathione dependent (49). We therefore investigated whether a similar requirement was necessary for the interference mediated by Hsp27 toward the detection of cytochrome *c* in the soluble fraction of cells exposed to staurosporine. The different L929 cell lines described above were then exposed for 18 h to 500 μM BSO, a γ-glutamyl synthetase-inhibiting agent. This treatment depleted intracellular reduced glutathione by more than 99% (not shown; see also references 58 and 60). As seen in Fig. 4D and E, the BSO treatment did not alter the ability of human Hsp27 to inhibit the staurosporine-induced appearance of cytosolic cytochrome *c*. Moreover, BSO did not significantly alter staurosporine ability to induce apoptosis in control L929-C2 cells, nor did it interfere with the protective activity mediated by Hsp27 (not shown). Similarly, the presence of the broad-range

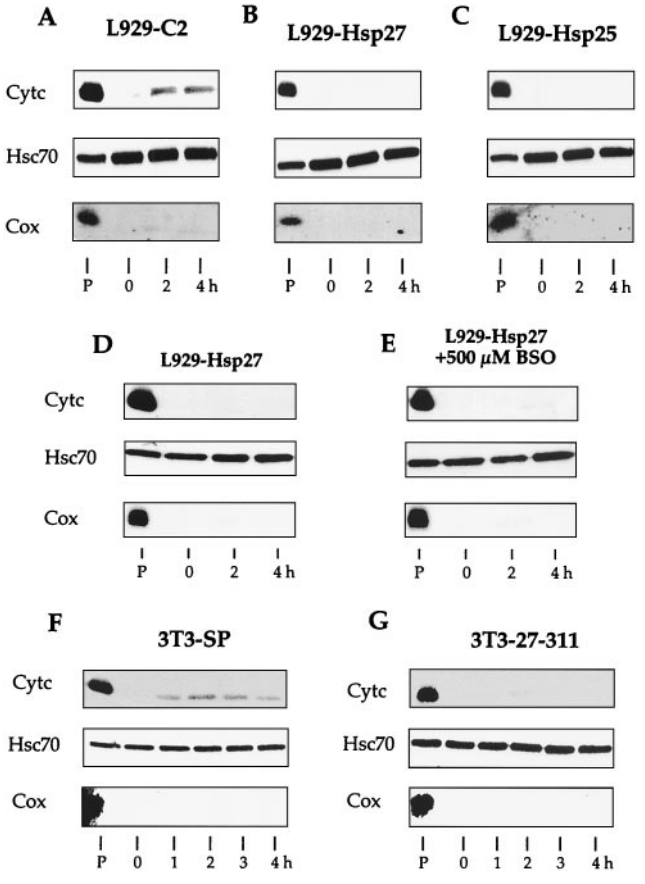

FIG. 4. Hsp27-mediated reduced accumulation of cytosolic cytochrome *c* is independent of apoptotic inducer, intracellular glutathione level, and cell line. (A to C) Analysis of cytochrome *c* release from mitochondria of control (L929-C2) (A), human Hsp27-expressing (L929-Hsp27) (B), and murine Hsp27-expressing (L929-Hsp25) (C) L929 cells treated for different times with 500 μM etoposide. (D and E) L929-Hsp27 cells exposed (E) or not (D) to 500 μM BSO for 18 h before being exposed (2 and 4 h) or not to 1 μM staurosporine. (F and G) Control (3T3-SP) (F) or human Hsp27-expressing (3T3-27-311) (G) NIH 3T3 cells either untreated or treated for various times with 1 μM staurosporine. Cells were lysed as described above in the legend to Fig. 2 and Materials and Methods to obtain a supernatant and pellet fraction. Cytochrome *c*, Hsc70, and Cox in the particulate and supernatant fractions were determined by immunoblot analysis using the corresponding antibodies. Autoradiographs of ECL-revealed immunoblot are presented. Lanes: P, pellet from untreated cells; 0 to 4, soluble fractions isolated from either untreated cells (0) or cells treated for the indicated number of hours with staurosporine or etoposide.

caspase inhibitor z-VAD-fmk in the culture medium of L929-Hsp27 cells exposed to staurosporine did not alter the Hsp27-mediated reduced detection of cytochrome *c* in the cytosol (not shown).

We also analyzed whether the effects described above were specific or not to L929 cells. This was assessed by using human Hsp27-expressing NIH 3T3 fibroblasts which, similarly to L929 cells, do not constitutively express detectable levels of endogenous murine Hsp27 under normal growth conditions. It is seen in Fig. 4F and G that human Hsp27 efficiently inhibited the detection of cytochrome *c* in the cytosol of NIH 3T3 cells exposed to staurosporine treatment. Analysis of the pellet fractions also confirmed that, in NIH 3T3 cells, human Hsp27 induced cytochrome *c* to remain associated with the mitochondrion-containing pellet resulting from centrifugation at 14,000 × *g* (not shown).

Taken together, our results suggest that the interference of Hsp27 toward the accumulation of soluble cytochrome *c* is not specific to a peculiar cell line or apoptotic inducer. Moreover, this activity is caspase-independent and not related to the already-described Hsp27 activity toward glutathione (59).

Enhanced kinetics of cytochrome *c* accumulation in the cytosol and caspase 3 activation in HeLa cells underexpressing Hsp27. Since HeLa cells constitutively express endogenous human Hsp27, we analyzed whether a decrease in the level of this protein could modify the kinetics of the staurosporine-induced appearance of cytochrome *c* in the cytosol. Using an antisense strategy, we generated HeLa cell lines that showed a decreased level of Hsp27 (see Materials and Methods). For example, HeLa-ASHsp27-1 cells (expressing 2.4 ng of Hsp27 per μg of total proteins) displayed a 40% reduced level of Hsp27 compared to control HeLa-neo15 cells (expressing 4 ng of Hsp27 per μg of total proteins, that is, at least four times more than L929-Hsp27 cells) (Fig. 5A) or the parental HeLa cells (not shown). Control experiments also showed that the accumulation of Hsp27 during heat shock recovery was reduced in HeLa-ASHsp27 cells. As shown in Fig. 5B, HeLa-ASHsp27-1 cells were more sensitive to staurosporine-induced apoptosis than the control cells, hence suggesting a physiological antiapoptotic role of endogenous Hsp27 in these cells. Analysis of the kinetics of cytochrome *c* accumulation in the cytosolic fraction revealed a strong effect that correlated with the decrease in Hsp27 expression. Indeed, in control and parental cells, cytochrome *c* began to be faintly detectable in the soluble cytoplasm after 4 h of staurosporine treatment while this protein was detected already after 1 h of treatment in HeLa-ASHsp27-1 cells (Fig. 5C and D). We also observed a more intense activation of DEVD-dependent procaspase 3-like protease in HeLa cells containing a reduced level of Hsp27 as analyzed using DEVD-AFC fluorogenic peptide (Fig. 5E). Immunoblot analysis of p17 cleavage polypeptide of procaspase 3 confirmed the more intense activation of this caspase in HeLa-ASHsp27-1 cells (Fig. 5F). Similar results were observed when other Hsp27 underexpressing (HeLa-ASHsp27-2) or control cell lines were analyzed or when HeLa cells were exposed to other apoptotic inducers, such as anti-Fas agonist antibody plus actinomycin D (not shown). Hence, a constitutive expression of human Hsp27 may act as a barrier against apoptosis by interfering with the appearance of cytosolic cytochrome *c* leading to reduced activation of caspases.

Hsp27 interferes with the release of cytochrome *c* from mitochondria. Several hypotheses can explain the data presented above. (i) Hsp27 interferes with the release of cytochrome *c* from mitochondria either by a physical interaction with mitochondria or by interfering with an upstream signal. (ii) As soon as it is released from mitochondria, cytochrome *c* interacts with Hsp27 and forms large complexes that are recovered in the fraction resulting from centrifugation at 14,000 × *g*. The second possibility is based on the fact that Hsp27 can interact with cytochrome *c* once it is released from mitochondria (9).

To approach the inhibitory mode of action of Hsp27 toward the presence of cytosolic cytochrome *c*, several control experiments have been performed. As mentioned above (Fig. 2B),

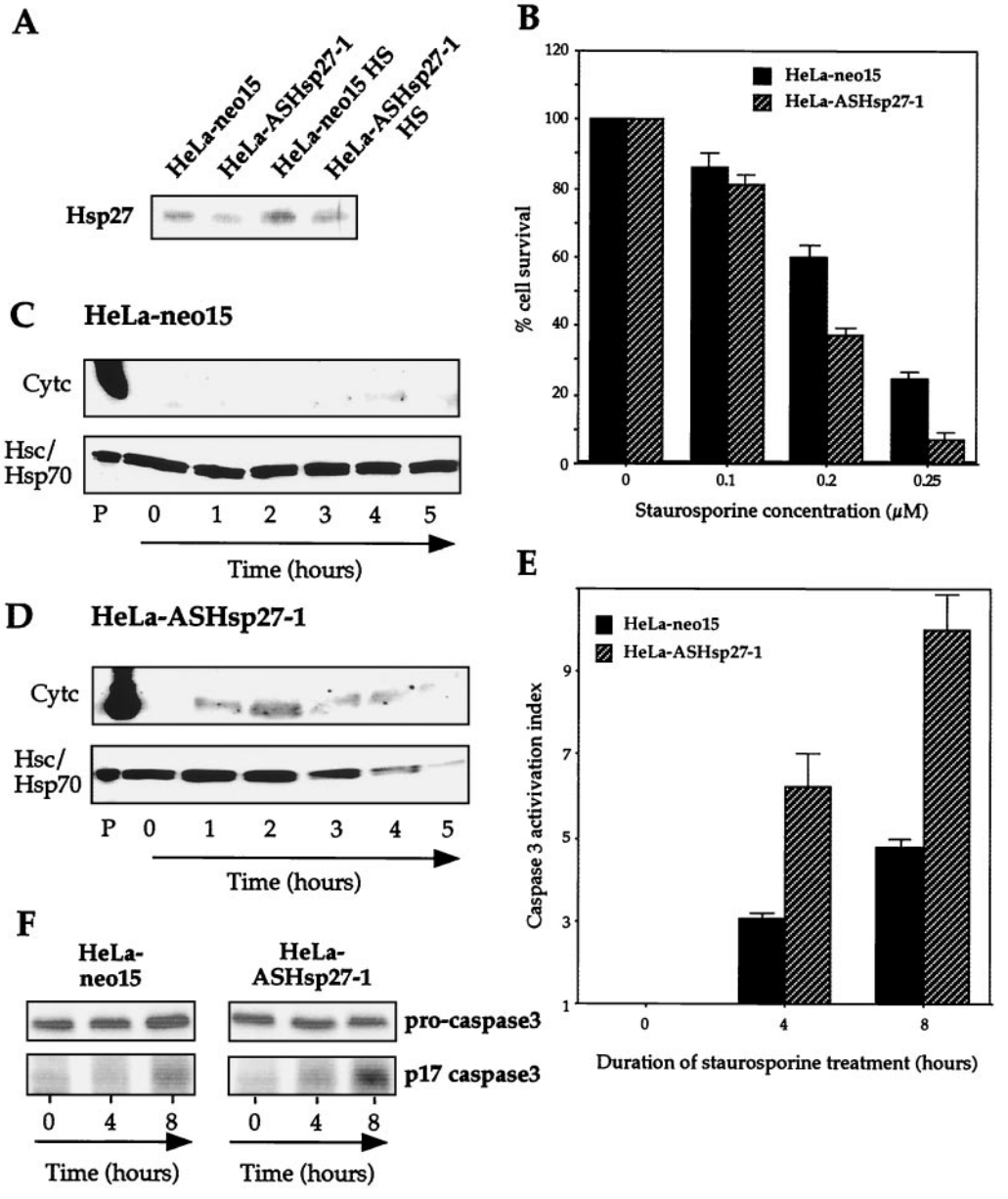

FIG. 5. Underexpression of Hsp27 in HeLa cells stimulates the accumulation of cytosolic cytochrome *c* and caspase 3 activation. (A) Analysis of human Hsp27 level present in HeLa-neo15 and HeLa-ASHsp27-1 cells kept at 37°C or treated (HS) for 90 min at 43°C and allowed to recover for 16 h. (B) Analysis of the resistance of HeLa cell lines to staurosporine. Cells were plated in 96-well tissue culture plates and allowed to grow for an additional 24-h period before being treated for 18 h with increasing concentrations of staurosporine (0 to 0.25 μM). Cellular survival was determined by crystal violet assay as described in Materials and Methods. The values were normalized to 100% using the cells not treated with staurosporine. Standard deviations (error bars) are indicated ($n = 3$). (C and D) Immunoblot analysis of cytochrome *c* release in cytosol. HeLa-neo15 cells (C) and HeLa-ASHsp27-1 (D) cells either kept untreated or treated for various times with 0.125 μM staurosporine were lysed as described in the legend for Fig. 2 to obtain a supernatant and pellet fraction. Lanes: P, pellet from untreated cells; 0 to 5, soluble fractions isolated from either untreated cells (0) or cells treated for the indicated number of hours with staurosporine. Hsc70 was used as an internal marker of gel loading. (E) Activity of DEVD-specific caspases in HeLa-neo15 and HeLa-ASHsp27-1 cells exposed or not to 0.125 μM staurosporine. The caspase activation index was determined as the ratio between the activity in extracts of treated cells to that measured in extracts of nontreated cells. The histogram shown is representative of three identical experiments; standard deviations (error bars) are presented ($n = 3$). (F) Immunoblot analysis of caspase 3 cleavage. Total protein extracts from HeLa-neo15 and HeLa-ASHsp27-1 cells either kept untreated (0) or treated for various times (4 and 8 h) with 0.125 μM staurosporine were analyzed in immunoblots probed with anti-caspase 3 antiserum which recognizes the uncleaved from of procaspase 3 as well as the p17 cleavage product. Autoradiographs of ECL-revealed immunoblots are presented.

the level of cytochrome *c* present in the pellet fraction resulting from centrifugation at 14,000 × *g* isolated from L929-Hsp27 cells exposed to staurosporine remained constant. The same holds true for the low level of Hsp27 present in this pellet fraction (not shown). This suggests that the retention of cytochrome *c* in the pellet resulting from centrifugation at 14,000 × *g* does not require a drastic increase in the level of Hsp27 present in this particulate fraction. In order to determine if the

low level of Hsp27 present in the pellet resulting from centrifugation at 14,000 × *g* could entrap cytochrome *c* at the surface of mitochondria or in structures that are recovered in the pellet resulting from centrifugation at 14,000 × *g*, the subcellular distribution of Hsp27 was analyzed in cells lysed in absence of detergent (see Materials and Methods). It can be seen in the immunoblot analysis presented in Fig. 6A that the vast majority of murine Hsp27 molecules was recovered in the soluble S10(1) supernatant (which represents the soluble fraction of the cytoplasm of L929-Hsp25 cells). The level of murine Hsp27 was very low in the P10(2) pellet, suggesting that, in these cells, this protein is not significantly associated with mitochondria. A similar intracellular distribution of human Hsp27 expressed in HeLa (Fig. 6B) or L929-Hsp27 (not shown) cells was observed. In contrast, mitochondrial marker proteins such as the β subunit of ATP synthase F1 complex, cytochrome *c*, and Cox (not shown) were recovered in the pellet fractions, particularly P10(2), which is enriched in mitochondria. The absence of mitochondrial marker proteins in the S10(2) supernatant is an argument in favor of the presence of intact mitochondria in the P10(2) pellet. Bcl-2, an antiapoptotic protein which is localized in the outer mitochondrial membrane as well as in the nuclear and endoplasmic reticular membranes (24, 51), was also recovered in the mitochondrial P10(2) fraction as well as in all the other membranous pellets. Hence, in L929 and HeLa cells, only a very small fraction of murine and human Hsp27 polypeptides copurified with mitochondria, and this was even after staurosporine treatment. Analysis of cytochrome *c* also revealed that its distribution in L929-Hsp25 cells was not significantly altered by 2 h of treatment with staurosporine (Fig. 6A).

We next performed confocal analysis of double staining experiments allowing for the simultaneous detection of cytochrome oxidase (Cox) revealed by a TRITC conjugate (red fluorescence) and human Hsp27 revealed by a FITC conjugate (green fluorescence). Computerized image analysis confirmed that only a small fraction of Hsp27 molecules was in the vicinity of mitochondria in the cytosol of HeLa and L929 cells. An illustration is presented in Fig. 6C, which shows a profile of Hsp27 and Cox fluorescence from HeLa cells exposed to 0.125 μM staurosporine.

We also performed confocal immunofluorescence analysis of the intracellular distribution of cytochrome *c* in control or Hsp27-expressing L929 cells treated or not for 3 h with 1 μM staurosporine. It is seen in the immunostaining analysis presented in Fig. 7 that in untreated control L929 cells, cytochrome *c* antibody displayed a reticular staining which is characteristic of the presence of this protein in mitochondria. Following staurosporine treatment, some cytochrome *c* staining was still observed in the reticular structures but a diffuse cytoplasmic staining was also observed. This diffuse staining was also clearly visualized using classical immunofluorescence analysis (not shown). When the same type of experiment was performed with L929-Hsp27 cells, no significant change in the reticular staining of cytochrome *c* was induced by staurosporine. This observation favors the hypothesis that Hsp27 interferes with the release of cytochrome *c* from mitochondria instead of entrapping this apoptogenic protein in large structures recovered in the particulate fractions following cell lysis.

Another experiment was performed to further exclude the possibility that Hsp27 entraps cytochrome *c* in large aggregates recovered in the pellet resulting from centrifugation at 14,000 × *g*. HeLa-neo15 cells were treated for 2 h with 0.125 μM staurosporine. Under these conditions, cytochrome *c* was not released in the cytosol and remained associated with the 14, 000 × *g* pellet (Fig. 5C). Cells were lysed in the presence of 0.1% NP-40 in order to solubilize cytoplasmic aggregates and to destroy mitochondria, leading most of cytochrome *c* to be recovered in the soluble cell lysate. Immunoprecipitations carried out with nonimmune or Hsp27 antibody were further analyzed in immunoblots probed with cytochrome *c* antibody. As we already described (9), some cytochrome *c* coimmunoprecipitated with Hsp27 (Fig. 8A). However, analysis of the supernatant after the immunoprecipitation step revealed that an almost complete immunodepletion of Hsp27 did not correlate with detectable immunodepletion of cytochrome *c* (Fig. 8B). This analysis, which was not performed in our previous report (9), suggests that only a very small fraction of total cytochrome *c* interacts with Hsp27. A similar observation was made when the experiment was performed with the detergent-solubilized pellets resulting from centrifugation at 14,000 × *g* (not shown). Another analysis was performed using HeLa-ASHsp27-1 cells treated for 2 h with staurosporine. Under these conditions a large fraction of cytochrome *c* was released from mitochondria and recovered in the cytosol centrifuged at 14,000 × *g* (Fig. 5D). Immunoprecipitation analysis of this 14,000 × *g* cytosol revealed that cytochrome *c* is present among the proteins immunoprecipitated by anti-Hsp27 antibody (Fig. 8C). However, analysis of the supernatants after the immunoprecipitation steps revealed once again that only a very small fraction of cytochrome *c* released from mitochondria interacts with Hsp27 (Fig. 8D). A similar observation was made after 4 h of staurosporine treatment (Fig. 8E). This excludes the possibility that all the cytochrome *c* molecules released from mitochondria could be bound to Hsp27 and entrapped in large cytoplasmic aggregates.

Hsp27 interferes with Bid intracellular redistribution. In order to better understand the mechanism of action of Hsp27 that delays the release of cytochrome *c* from mitochondria, we investigated whether the expression of this stress protein interfered with Bid, a polypeptide which shows a drastic intracellular redistribution when cells are exposed to an apoptotic stimulus. Indeed, Bid, which is mainly cytoplasmic, concentrates at the level of mitochondria in cells exposed to staurosporine; a phenomenon which destabilizes Bax and Bak and induces cytochrome *c* release (11, 22, 39, 42, 44, 79). We have tested the presence of Bid in the cytosol of control HeLa-neo15 and Hsp27 underexpressing HeLa-ASHsp27-1 cells exposed or not to 0.125 μM staurosporine. It is seen in the immunoblot analysis presented in Fig. 9 that, in HeLa-neo15 cells, at least 3 h of treatment with staurosporine was necessary to observe a decrease in the level of cytosolic Bid. The decrease was more pronounced after 4 h (not shown), when cytochrome *c* began to be released from mitochondria (Fig. 5C). When HeLa-ASHsp27-1 cells were analyzed, the kinetics of disappearance of Bid from the cytosol was more rapid and occurred already after 1 h of treatment; this phenomenon correlated again with the beginning of the release of cytochrome *c* from mitochondria. Control experiments showed that the intracellular locale of other cytosolic proteins such as

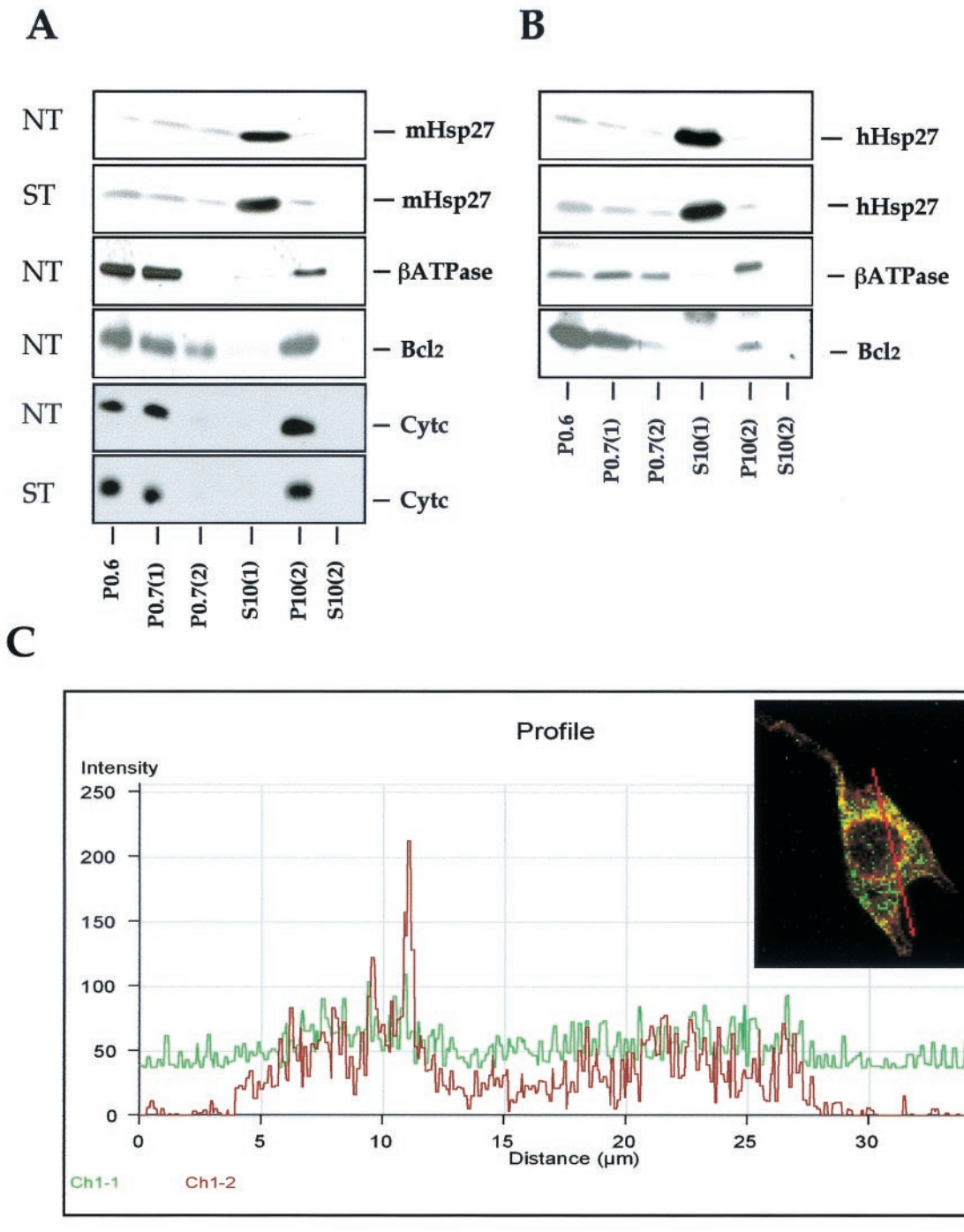

FIG. 6. The majority of the cellular content of Hsp27 is localized in the soluble cytoplasm. (A) Analysis of murine Hsp27 intracellular localization. L929-Hsp25 cells, either grown under normal conditions (NT) or treated (ST) for 2 h with 1 μM staurosporine, were lysed and fractionated as described in Materials and Methods. Immunoblot analysis of the different subcellular fractions was performed with antisera that specifically recognize murine Hsp27, ATP synthase β subunit (βATPase), Bcl-2, and cytochrome *c*. (B) Same as panel A, but here the intracellular localization of human Hsp27 constitutively expressed in HeLa cells treated or not for 2 h with 0.125 μM staurosporine was analyzed. (C) Comparison of Hsp27 and mitochondrial localization by confocal microscopy analysis. Hsp27 and Cox fluorescence was analyzed in HeLa cells treated for 4 h with 0.125 μM staurosporine. Cells were stained for Hsp27 (green fluorescence) and Cox (red fluorescence) and processed for confocal analysis as described in Materials and Methods. The fusion image (merge) is shown. The graph represents the fluorescence distribution of Hsp27 (green; Ch1-1) and Cox (red; Ch1-2) determined for the section of the cell shown in the green/red fusion image. Results are representative of three independent experiments.

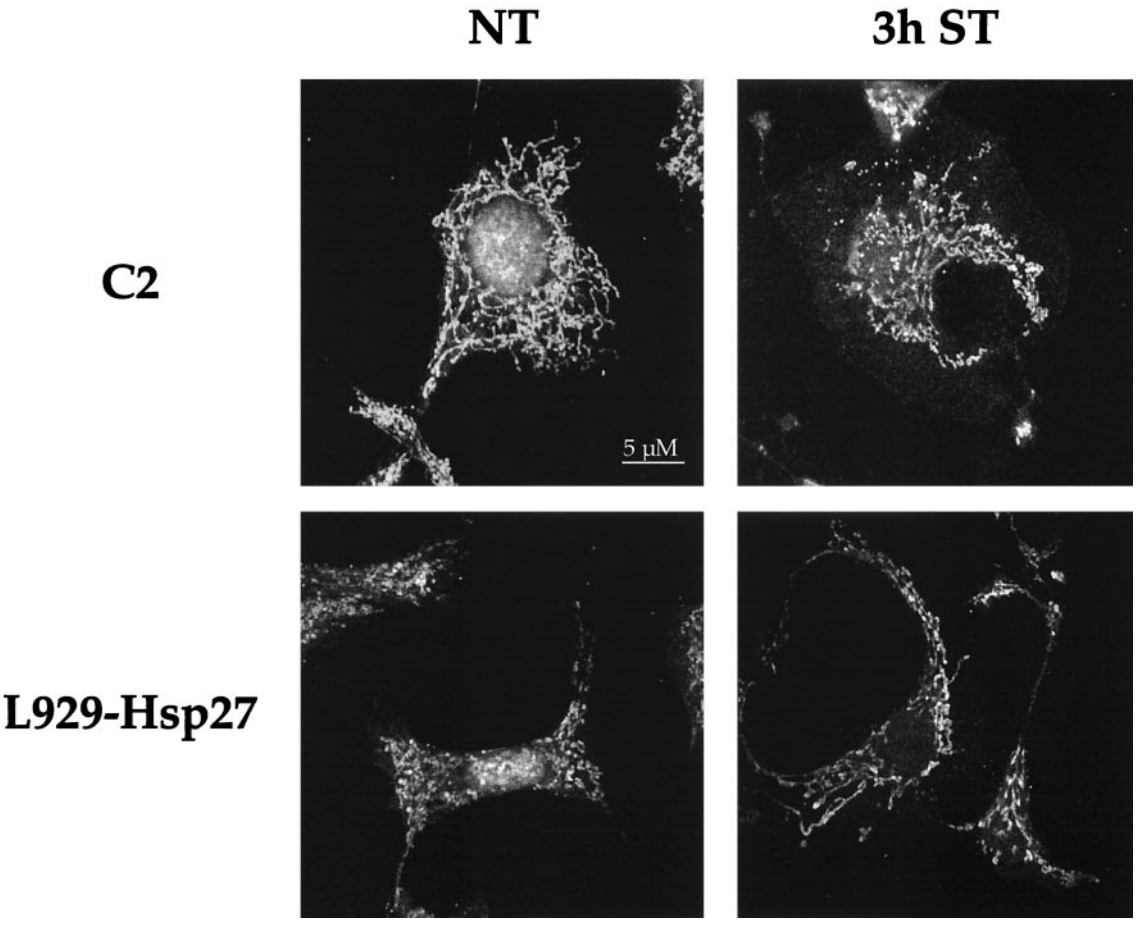

FIG. 7. Confocal microscopy analysis of cytochrome *c* immunostaining in control and Hsp27-expressing L929 cells exposed or not to staurosporine. Control L929 cells (C2) and L929-Hsp27 cells were either kept untreated (NT) or treated for 3 h with 1 μM staurosporine (3 h ST). Cells were prepared for immunostaining analysis using anti-cytochrome *c* antibody and observed under a confocal fluorescence microscope as described in Materials and Methods.

the stress proteins Hsc70 and Hsp70 was not modified by a similar staurosporine treatment (Fig. 9). We next analyzed whether the modulation of Bid intracellular localization by Hsp27 was a consequence of the formation of Bid-Hsp27 complexes. Coimmunoprecipitation analysis revealed that in our cell system Hsp27 does not bind Bid or even Bax, which resides downstream of Bid (not shown).

In L929-C2 cells exposed to staurosporine or etoposide, Bid also had the tendency to disappear from the cytosolic fraction and to be recovered, at least in part, as a full-length Bid polypeptide in the pellet fraction (Fig. 10). We did not detect the 15-kDa cleaved fragment of Bid (39, 42). However, due to the weak efficiency of the Bid antibody in murine cells, it is still possible that in our experiments a fraction of Bid was cleaved and not detected. In contrast, no significant redistribution of Bid was observed in L929-Hsp27 cells exposed to staurosporine or etoposide (Fig. 10).

Hence, in staurosporine- or etoposide-treated cells, the inhibitory effect of Hsp27 toward cytochrome *c* release probably results from interference with signaling pathways residing upstream of Bid.

F-actin network as a potential upstream target protected by Hsp27. As an approach toward identifying pathways upstream of Bid that could be modulated by Hsp27, we have analyzed whether the well-known activity of Hsp27 as a modulator of F-actin network (19, 36) could be related to its negative effect against cytochrome *c* release from mitochondria. This was performed by monitoring the presence of cytochrome *c* in the soluble cytoplasm at various times, before and after adding a 0.5 μM concentration of the actin microfilament depolymerizing agent cytochalasin D to the culture medium of control L929-C2 cells. This treatment efficiently dismantled F-actin architecture in these cells (see Fig. 13B). It is seen in the immunoblots presented in Fig. 11A that cytochalasin D specifically induced the release of cytochrome *c* in the cytosol of L929-C2 cells. The release was maximal after 6 h of treatment. Similar results were observed in L929-C3 cells (not shown). In contrast, cytochrome *c* release was strongly attenuated when the same experiment was performed using L929-Hsp27 cells. Analysis of the other L929 cell lines expressing different levels of murine Hsp27 (not shown) led to the conclusion that the delay in cytochrome *c* release was dependent on the level of Hsp27 expression. Immunofluorescence analysis also revealed that a fraction of total cytochrome *c* was released from mitochondria and displayed a diffuse cytoplasmic localization; a

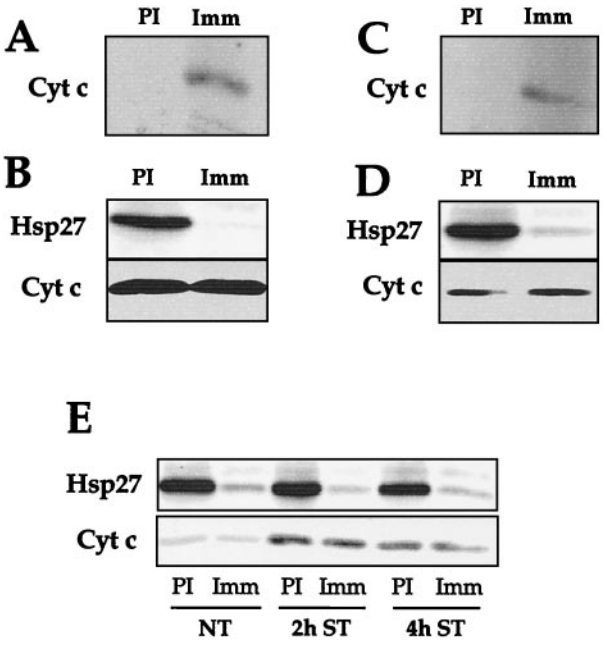

FIG. 8. Analysis of the interaction of Hsp27 with cytochrome *c*. (A) Immunoblot analysis of the proteins immunoprecipitated by anti-Hsp27 antibody. HeLa-neo15 cells, treated for 2 h with 0.125 μM staurosporine, were lysed in the presence of 0.1% NP-40 as described in Materials and Methods. This protocol destroyed mitochondria, leading most cytochrome *c* to be recovered in the soluble cell lysate. Immunoprecipitations were carried out with nonimmune (PI) or Hsp27 (Imm) antibody, and the immunoprecipitated proteins were analyzed in immunoblots probed with anti-cytochrome *c* antibody. Note that some endogenous cytochrome *c* coimmunoprecipitates with Hsp27. (B) Analysis of the relative fraction of endogenous cytochrome *c* that coimmunoprecipitates with Hsp27. HeLa-neo15 cells were treated and lysed in detergent, and immunoprecipitations carried out as above. In this case, the proteins present in the supernatants obtained from the immunoprecipitation step were analyzed in immunoblots probed with both Hsp27 and cytochrome *c* antisera. Note that no detectable decrease in the level of endogenous cytochrome *c* is observed after a complete immunodepletion of Hsp27. (C) Same as panel A, but in this case HeLa-ASHsp27-1 cells treated for 2 h with 0.125 μM staurosporine were lysed using the method that preserves mitochondrial integrity. A supernatant and a pellet fraction resulting from centrifugation at 14,000 × *g* were obtained as described in Materials and Methods. We have used the supernatant obtained from centrifugation at 14,000 × *g* as the starting material in order to analyze Hsp27 interaction with cytochrome *c* once it is released from the mitochondria. Immunoprecipitations were carried out as described above with nonimmune (PI) or Hsp27 (Imm) antibody, and the immunoprecipitated proteins were analyzed in immunoblots probed with anti-cytochrome *c* antibody. Note the coimmunoprecipitation of cytochrome *c* released from mitochondria with Hsp27. (D) In this case, the supernatants obtained following the immunoprecipitation step performed in panel C were analyzed in immunoblot probed with both Hsp27 and cytochrome *c* antisera. Once again no detectable decrease in the level of cytochrome *c* is observed after an almost complete immunodepletion of Hsp27. (E) Same as panel D, except that HeLa cells were either nontreated (NT) or treated for 2 or 4 h with 0.125 μM staurosporine. Autoradiographs of immunoblots are presented. This experiment indicates that only a minor fraction of total mitochondria or mitochondria released cytochrome *c* can interact with Hsp27.

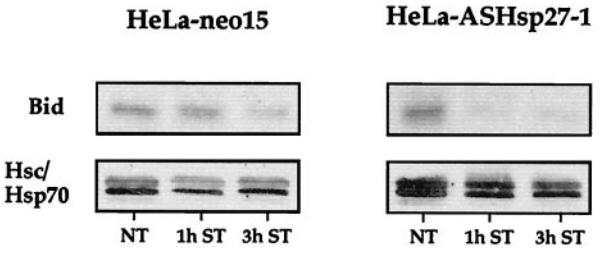

FIG. 9. Analysis of Bid present in the cytosol of HeLa-neo15 and HeLa-ASHsp27-1 cells kept either untreated (NT) or exposed to 0.125 μM staurosporine for 1 h (1 h ST) or 3 h (3 h ST). Cells were lysed under conditions which preserve mitochondrial and membrane integrity, and the cytosolic supernatant resulting from centifugation at 20,000 × *g* was analyzed (as described in Materials and Methods). Total cytosolic extracts were analyzed in immunoblots probed with anti-Bid or anti-Hsc70/Hsp70 antibody. Control experiments showed that the supernatants were devoid of Cox immunoreactivity (not shown). Autoradiographs of ECL-revealed immunoblots are presented.

phenomenon not observed in L929 cells expressing Hsp27 (not shown).

We also investigated whether the cytochalasin D induction of cytochrome *c* release was time correlated with the activation of procaspase 3. As seen in Fig. 11B, DEVD-dependent caspase 3-like proteases begin to be activated after 3 h of treatment with cytochalasin D. This period corresponded with the release of cytochrome *c* in the cytosol (Fig. 11A). After 6 h of treatment with cytochalasin D, the caspase 3-like activation index was 1.4 and increased to 2.7 after 9 h of treatment (Fig. 11B). In cells expressing human Hsp27, no activation was detectable after 3 h of treatment, and the activation index was only of 1.4 after 9 h of treatment. Analysis of procaspase 8 revealed that this protease is activated by cytochalasin D but at a later time than procaspase 3 (Fig. 11C). This suggests that caspase 8 activation may occur downstream of procaspase 3 activation.

Analysis of Bid intracellular localization in control L929-C2 cells revealed that already after 2 h of cytochalasin D treatment this protein had the tendency to redistribute from the cytosol to the particulate fractions (Fig. 11D). Analysis of the mitochondrial P10(2) fraction (Fig. 6A) revealed an increased level of Bid in this fraction in cells exposed to cytochalasin D (not shown). This suggests that at least a fraction of Bid translocates from the cytosol to the mitochondria. No significant change in Bid subcellular distribution was observed in L929-Hsp27 cells exposed to cytochalasin D (Fig. 11D). These results suggest that cytochalasin D stimulates a Bid-mediated mitochondrial cytochrome *c* loss and subsequently procaspase 3-like activation. This cascade of events is strongly attenuated by the presence of 0.9 ng of Hsp27 per μg.

Control experiments were also performed in order to assess that the release of cytochrome *c*, and the activation of caspase 3 in cells exposed to cytochalasin D was not due to a side effect induced by this drug toward cellular targets other than F-actin microfilaments. To do so, cells were pretreated for 1 h with a 2 μM concentration of the F-actin stabilizing agent phalloidin before being exposed or not to 0.5 μM cytochalasin D for different times. As already described (41), the phalloidin pretreatment reduced the F-actin dismantling activity of cytochalasin D (not shown). Under these conditions, the ability of cytochalasin D to induce the release of cytochrome *c* from mitochondria (at least during the first 6 h of the treatment) was strongly attenuated (Fig. 12A). Moreover, a drastic decrease in

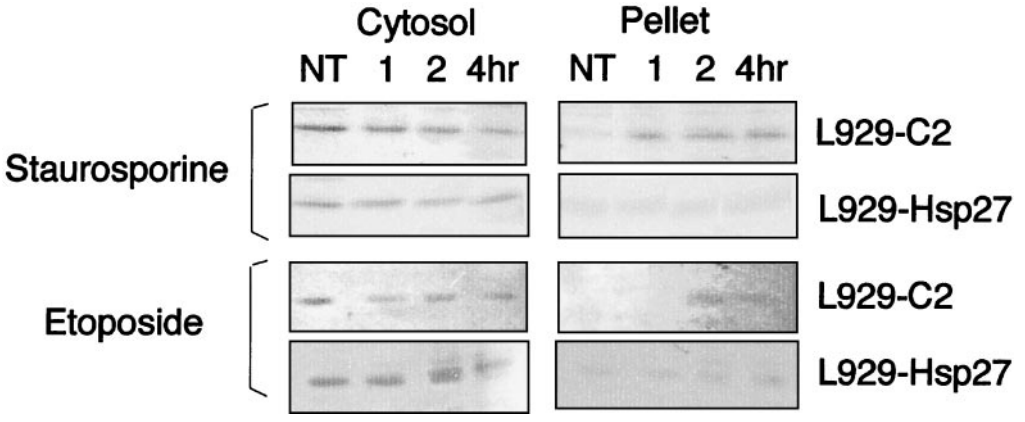

FIG. 10. Hsp27 expression interferes with the staurosporine- and etoposide-induced Bid intracellular relocalization in murine L929 cells. Control L929-C2 and Hsp27-expressing L929-Hsp27 cells kept either untreated (NT) or exposed to staurosporine (1 μM) or etoposide (500 μM) for either 1, 2, or 4 h were lysed under conditions which preserve mitochondrial and membrane integrity as described in Materials and Methods. The resulting P20 and S cytosolic fractions were analyzed in immunoblots probed with anti-Bid antibody. Autoradiographs of immunoblots are shown.

the activation of procaspase 3 (about 60%) was also observed in cells pretreated with phalloidin (Fig. 12C). This confirmed that the destruction of F-actin by cytochalasin D triggers an apoptotic signal that induces the release of cytochrome *c* from mitochondria and subsequently caspase 3 activation. A similar analysis was performed in staurosporine-treated cells. It is seen in Fig. 12B that phalloidin reduced (by a factor of about 20 to 30%) the effectiveness of staurosporine to induce cytochrome *c* release. Moreover, phalloidin reduced by about 30% the activation of DEVD-dependent procaspase 3-like protease by staurosporine (Fig. 12D). This suggests that the destruction of F-actin in staurosporine-treated cells participates to a certain extent in the triggering of cytochrome *c* release and procaspase activation. In contrast, in etoposide-treated cells, the F-actin network was not altered (at least during early apoptotic response) (Fig. 13D). In this case, a phalloidin pretreatment of the cells had no significant effect on the kinetics of cytochrome *c* release (not shown) and DEVD-dependent procaspase 3-like activation (Fig. 12E).

Since cytochalasin D is a specific in vivo inhibitor of actin polymerization (81) and Hsp27 has been reported to delay its effectiveness (19, 35), control experiments were performed to analyze the degree of actin cytoskeleton destruction induced by cytochalasin D in L929 cells expressing or not human Hsp27. It is seen in the immunofluorescence analysis presented in Fig. 13 that a treatment for 2 h with 0.5 μM cytochalasin D efficiently dismantled actin microfilament architecture in control L929-C2 cells (Fig. 13A and B). This treatment corresponded with the beginning of the release of cytochrome *c* by mitochondria (not shown). In contrast, human Hsp27 expressing L929-Hsp27 cells, which display a more fusiform morphology (see references 58 and 59), showed an increased resistance to this phenomenon (Fig. 13E and F). Some protection was also observed in L929-Hsp25 cells expressing murine Hsp27 (0.45 ng/μg) (not shown). However, a lower level of murine Hsp27 expression (as, for example, in L929-Hsp25wt-1 cells) was unable to delay cytochalasin D efficiency. These observations confirm earlier observations that the level of expression of Hsp27 is an important parameter to generate a protection against F-actin disruption by cytochalasin D (19).

We also analyzed the organization of F-actin microfilaments in staurosporine-treated L929 cells. Of interest, a 2-h treatment of control L929 cells with a 1 μM concentration of this apoptotic agent induced a complete disappearance of F-actin stress fibers, but some junctional actin was still visible around the cells (Fig. 13C). Moreover, a pretreatment of the cells with 2 μM phalloidin reduced the disappearance of F-actin induced by staurosporine (not shown). In contrast, in L929-Hsp27 cells exposed to staurosporine, some F-actin fibers were still detectable (Fig. 13G) as well as junctional actin. It should nevertheless be noted that these cells had lost their fusiform appearance, probably because of the shortening of F-actin fibers. Treatment for shorter periods (30 min or 1 h) revealed that staurosporine was effective already after 30 min of treatment (not shown). These observations indicate that F-actin destruction by staurosporine is a very early event that is time correlated with the beginning of cytochrome *c* release (Fig. 2) and which occurs before caspase 3 activation (Fig. 1). When the different murine Hsp27-expressing cells were analyzed, we observed that a low level of murine Hsp27 expression (0.15 ng/μg; L929-Hsp25wt-1 cells) did not protect F-actin stress fibers from being destroyed by staurosporine. An intermediate level of protection was observed in cells expressing medium levels of murine Hsp27 (0.45 ng/μg; L929-Hsp25 cells) (not shown).

The same type of analysis was performed in cells exposed to etoposide. In these cells, no destruction of F-actin architecture was detected during the first hours of the treatment (Fig. 13D), and no effect of Hsp27 expression could be detected (Fig. 13H). This leads to the conclusion that in etoposide-treated cells Hsp27 acts at an other level to delay the release of cytochrome *c* from mitochondria.

Taken together, our results suggest that F-actin can act as an upstream target which, when altered (i.e., by cytochalasin D or staurosporine treatment), generates an apoptotic signal that activates cytochrome *c* release from mitochondria. Consequently, the Hsp27-mediated decrease in cytochrome *c* release

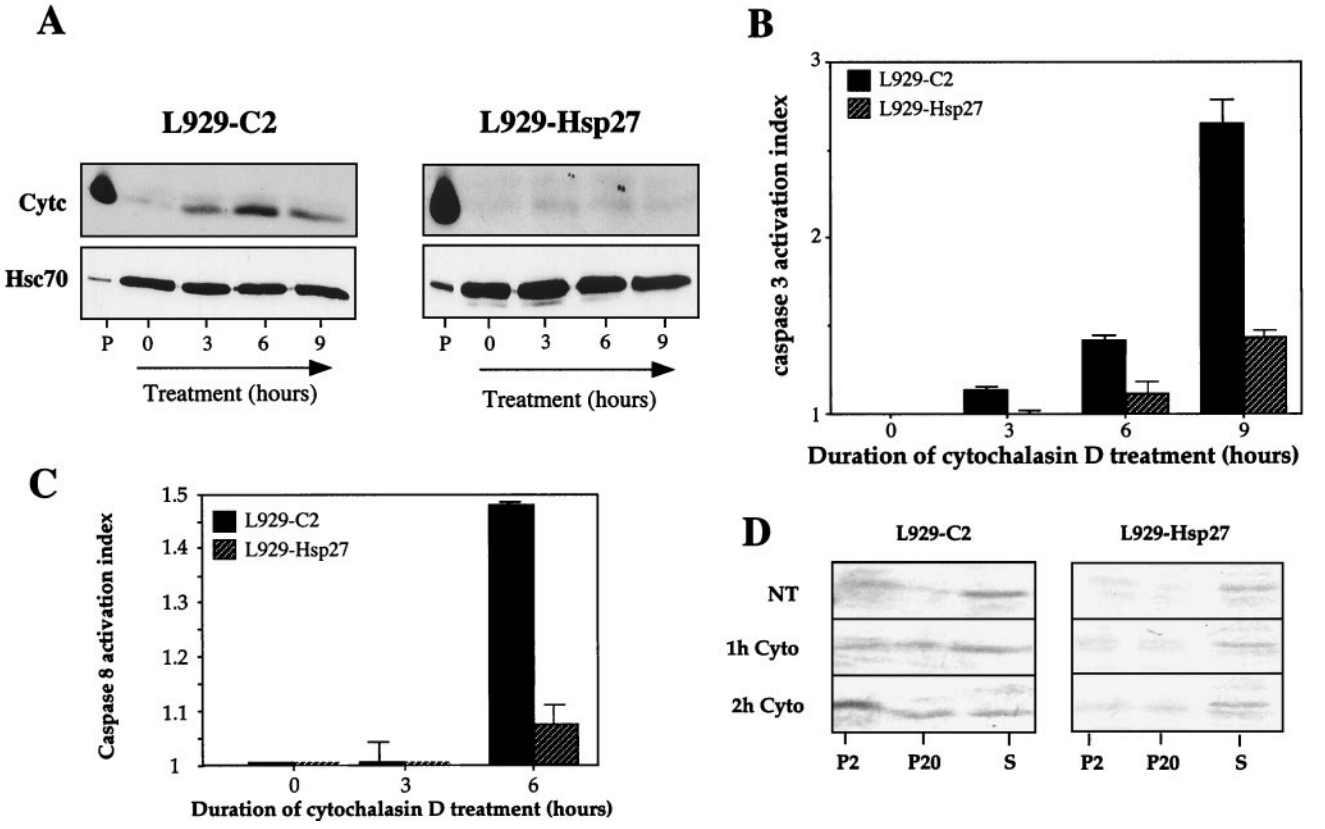

FIG. 11. Hsp27 expression interferes with cytochalasin D-induced release of cytochrome *c* and procaspase 3 activation. (A) Cytochrome *c* release analysis. Control (L929-C2) and human Hsp27-expressing (L929-Hsp27) cells were either kept untreated or treated for various times with 0.5 μM cytochalasin D. Cells were then processed, and proteins were analyzed in immunoblots as described in Materials and Methods and in the legends to Fig. 2 and 3. The presence of cytochrome *c* (Cytc) and Hsc70 in the different fractions is shown. Autoradiographs of ECL-revealed immunoblots are presented. Note that human Hsp27 strongly decreases the release of cytochrome *c* induced by cytochalasin D. Lanes: P, pellet from untreated cells; 0, 3, 6, and 9, soluble fractions isolated from untreated cells or cells treated for the indicated hours with cytochalasin D. (B) Caspase 3 activation by cytochalasin D. Control (L929-C2) and human Hsp27-expressing (L929-Hsp27) cells were treated as described above for panel A. Activity of DEVD-specific caspases was then measured using the fluorescent substrate DEVD-AFC as described in Materials and Methods. (C) Caspase 8 activation by 0.5 μM cytochalasin D. IETD-AFC activity was determined as described in Materials and Methods. The activation index was determined as the ratio between the activity in extracts of treated cells to that measured in extracts of nontreated cells. The histograms shown in panels B and C are representative of three identical experiments; standard deviations (error bars) are presented ($n = 3$). (D) Analysis of Bid localization in control L929-C2 and Hsp27-expressing L929-Hsp27 cells kept either untreated (NT) or exposed to 0.5 μM cytochalasin D for 1 h (1 h Cyto) or 2 h (2 h Cyto). Cells were lysed under conditions which preserve mitochondrial and membrane integrity and the resulting P2, P20, and S cytosolic supernatants were analyzed (as described in Materials and Methods). Autoradiographs of immunoblots probed with anti-Bid antibody are shown.

in cytochalasin D- and staurosporine-treated cells may result, at least in part, from the protective activity of this stress protein against F-actin network destruction. The inhibition of this apoptotic pathway also appears to depend on the level of Hsp27 required to maintain F-actin integrity.

DISCUSSION

We report that the expression of Hsp27 can delay the detection of soluble cytoplasmic cytochrome *c* in cells exposed to different apoptotic agents, such as staurosporine, etoposide, and cytochalasin D. This phenomenon was cell line, glutathione, and caspase independent and therefore not related to the Hsp27 protective activity against oxidative stress (59) or to the activation of caspases upstream of mitochondria (e.g., procaspase 8). Previously, we also reported that Hsp27 can delay cytochrome *c* release in thermotolerant cells reexposed to heat shock (67). We show here that the delay induced by Hsp27 correlated with its level of expression: for example, murine Hsp27 was not effective when its level was 0.15 ng/μg, but a three-times increase in its level delayed the detection of cytochrome *c* by several hours. In L929-Hsp27 cells which express a high level of human Hsp27 (0.9 ng/μg), soluble cytoplasmic cytochrome *c* was even more difficult to detect. We also analyzed HeLa cells that constitutively express a high level of endogenous human Hsp27. A 40% decrease in the level of this protein, generated through an antisense strategy, sensitized HeLa cells to staurosporine. This phenomenon was correlated with a more rapid detection of cytochrome *c* in the soluble cytoplasm and procaspase activation. This leads to the conclusion that the constitutive expression of Hsp27 in HeLa cells protects these cells against apoptosis.

How does Hsp27 act to specifically delay the detection of cytochrome *c* in the soluble cytoplasm of cells exposed to apoptotic agents? Several possibilities can be envisaged: Hsp27

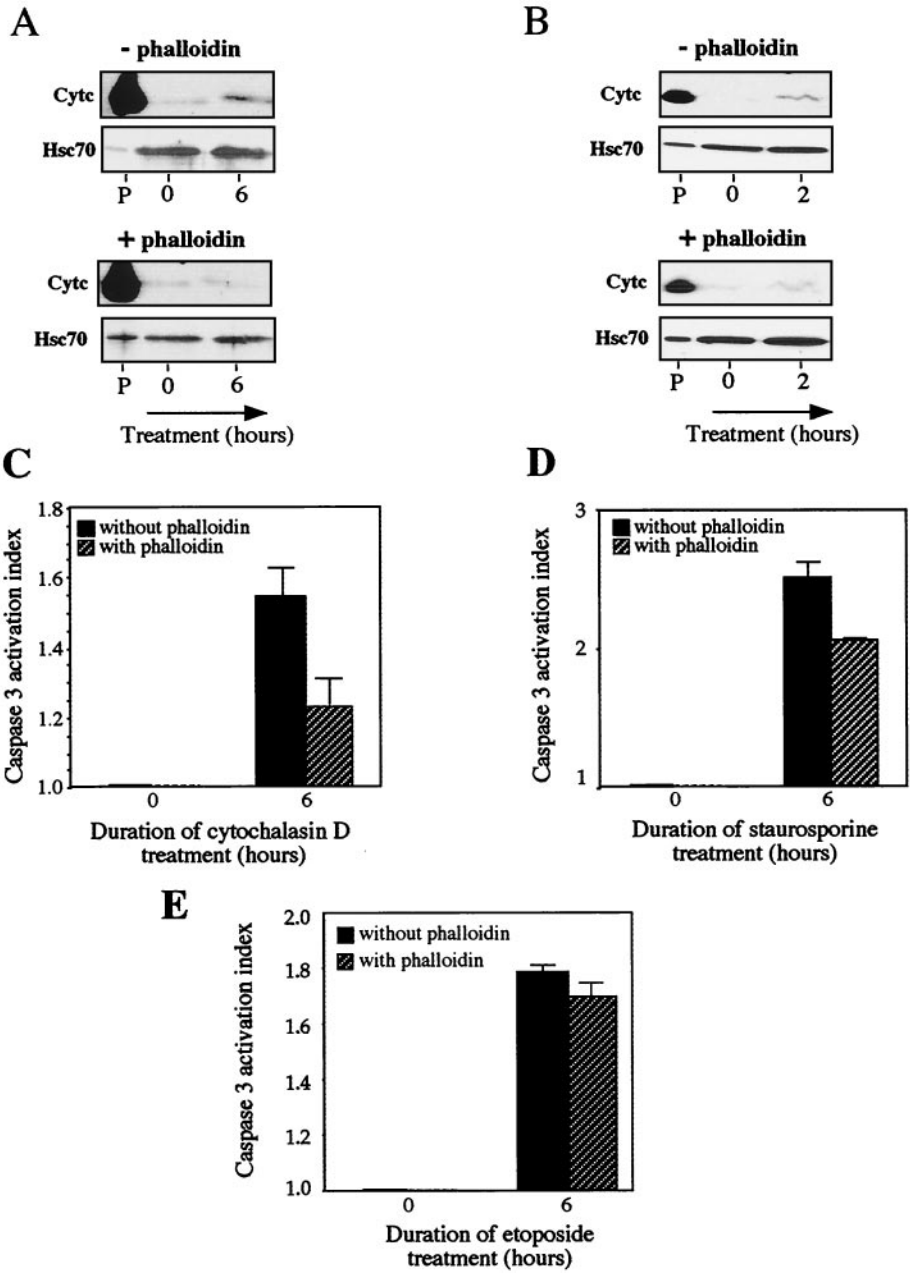

FIG. 12. Phalloidin counteracts the cytochalasin D-mediated release of cytochrome *c* from mitochondria and procaspase 3 activation. The effect is partial in case of staurosporine-treated cells. (A) Cytochrome *c* release analysis. Control (L929-C2) cells were either kept untreated or treated for 6 h with 0.5 μM cytochalasin D in the absence (−) or presence (+) of 2 μM phalloidin added to the culture medium 1 h before cytochalasin D. Cells were then processed for cytochrome *c* release analysis and proteins present in the different fractions were analyzed in immunoblots as described in Materials and Methods. The presence of cytochrome *c* (Cytc) and Hsc70 in the different fractions is shown. Autoradiographs of ECL-revealed immunoblots are presented. Note that phalloidin strongly decreases the release of cytochrome *c* induced by cytochalasin D. Lanes, P, pellet from untreated cells; lanes 0 and 6, soluble fractions isolated from untreated cells (0) or cells treated for 6 h with cytochalasin D. (B) Same as panel A, but in this case cells were treated with 1 μM staurosporine. (C) Caspase 3 activation in L929-C2 extracts isolated after 6 h of treatment with 0.5 μM cytochalasin D in the absence or presence of 2 μM phalloidin added to the culture medium 1 h before cytochalasin D. Activity of DEVD-specific caspases was then measured using the fluorescent substrate DEVD-AFC as described in Materials and Methods. (D) Same as panel C but in the presence of 1 μM staurosporine. (E) Same as panel C but in the presence of 500 μM etoposide. The activation index was determined as the ratio between the activity in extracts of treated cells to that measured in extracts of nontreated cells. The histogram shown is representative of three identical experiments; standard deviations (error bars) are presented ($n = 3$). Note the protective activity of phalloidin.

(i) induces the rapid degradation of cytochrome *c* once it is released from mitochondria, (ii) through its binding to cytochrome *c* (9) and its presence at the surface of mitochondria can inhibit the release of cytochrome *c* and/or can form large cytoplasmic aggregates that are recovered in the pellet resulting from centrifugation at 14,000 × *g* upon cell lysis, or (iii) interferes with an apoptotic signaling pathway upstream of mitochondria.

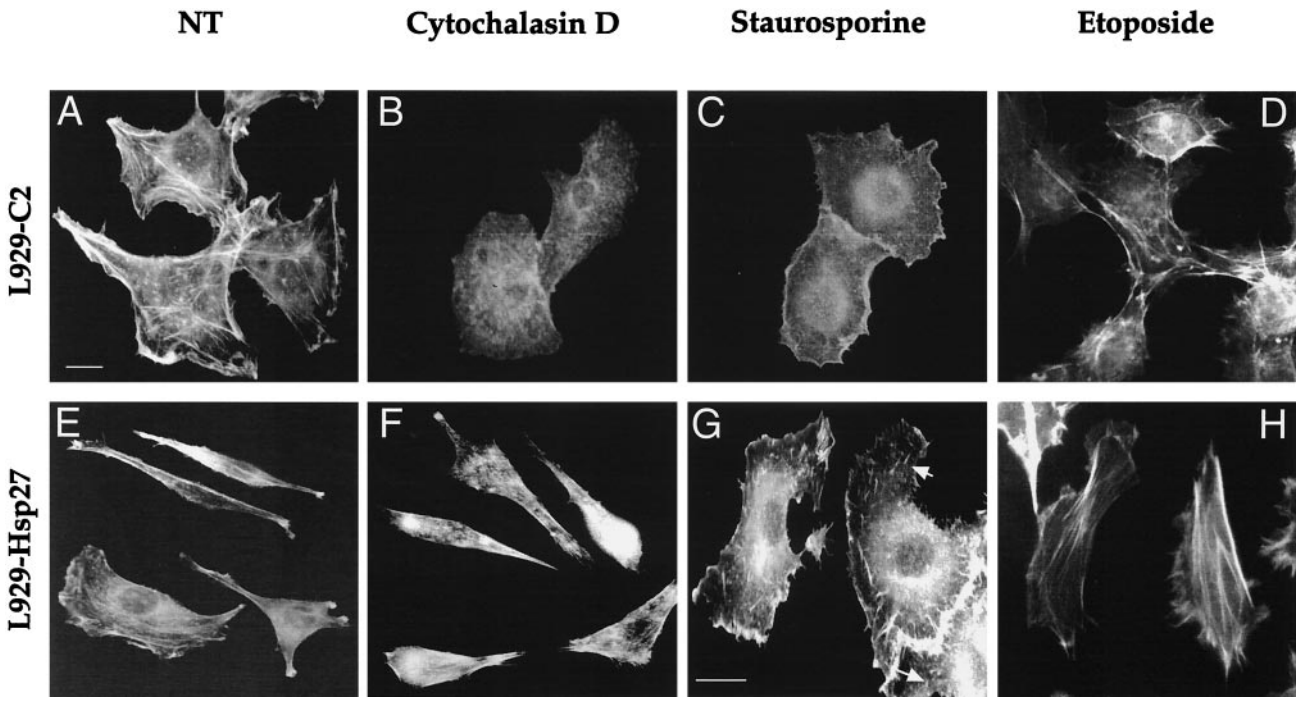

FIG. 13. Hsp27 expression interferes with cytochalasin D- and staurosporine-induced damages to F-actin. Fluorescence photomicrographs demonstrating the effect of cytochalasin D and staurosporine on F-actin fibers. Control L929-C2 cells (A to D) and human Hsp27-expressing L929-Hsp27 cells (E to H) were plated on glass plates and allowed to enter exponential cell growth phase for 24 h. They were then either kept untreated (A and E) or treated with 0.5 μM cytochalasin D (B and F), 1 μM staurosporine (C and G), or 500 μM etoposide (D and H). After 2 h of treatment the cells were fixed, stained with FITC-labeled phalloidin, and examined under a fluorescence microscope. The photomicrograph in panel G is enlarged in order to better detect the F-actin fibers (arrows), which are still visible in L929-Hsp27 cells treated with staurosporine. Bar, 10 μM.

Concerning the first possibility mentioned above, the unchanged level of cytochrome *c* present in the pellet isolated from L929-Hsp27 cells by centrifugation at 14,000 × *g* indicates that this protein remains associated with fast-sedimenting structures in staurosporine-treated cells. This excludes the possibility that cytochrome *c* is degraded as soon as it is released from mitochondria—a conclusion reinforced by experiments performed in the presence of the broad range caspase inhibitor z-VAD-fmk. The lack of effect of this inhibitor also suggests that Hsp27 has a specific inhibitory effect which does not depend on upstream caspase activation.

Concerning the second possibility, that the interaction of Hsp27 with cytochrome *c* (9) is responsible for the delayed release of cytochrome *c* from mitochondria, several points are not in favor of this possibility. First, the vast majority of Hsp27 is cytosolic (see reference 57). Second, in spite for the fact that Hsp27 interacts with cytochrome *c*, control experiments presented in this paper revealed that this assumption is true for only a very small fraction of cytochrome *c.* This observation is therefore not in favor of the formation of large Hsp27-cytochrome *c* complexes that could be recovered in the pellet resulting from centrifugation at 14,000 × *g* following cell lysis. Confocal immunofluorescence analysis of cytochrome *c* is also not in favor of the formation of such complexes and suggests that Hsp27 expression inhibits the release of cytochrome *c* from mitochondria. Could a minor and particular oligomeric form of Hsp27 interact with cytochrome *c* at the surface of mitochondria and interfere with its release in the cytoplasm? Concerning this possibility, we have already reported, using cell extracts incubated with atractyloside, that the small fraction of Hsp27 copurifying with the outer mitochondrial membrane does not appear to account for its antiapoptotic activity (9).

Concerning a possible interference mediated by Hsp27 at the level of an apoptotic signaling pathway residing upstream of mitochondria, this hypothesis is reinforced by the fact that Hsp27 modulates the Bid intracellular locale. Indeed, in HeLa cells, the underexpression of Hsp27 shortened the delay required to observe the disappearance of Bid from the cytosolic fraction. This delay was time correlated with the release of cytochrome *c* from mitochondria. Analysis of Bid in control and Hsp27-expressing L929 cells exposed or not to cytochalasin D, staurosporine, or etoposide revealed that in all the cases studied, Hsp27 interfered with the redistribution of Bid from the cytosol to the particulate fraction. Hence, the inhibitory effect of Hsp27 toward cytochrome *c* release probably results from altered signaling pathways residing at the level or upstream of Bid. Concerning a putative interaction of Hsp27 with Bid, coimmunoprecipitation analysis did not give positive results suggesting that these two proteins probably do not directly interact.

We next analyzed F-actin as a possible upstream target modulated by Hsp27. Relations between F-actin and apoptosis have been described in several cell systems, such as rat proximal tubular cells (75) and neutrophils (8). Here, we report that a short incubation of control cells with the F-actin depolymer-

izing agent cytochalasin D triggered cytochrome *c* release and procaspase 3-like activation. This phenomenon was strongly attenuated when cells were pretreated with the F-actin stabilizing agent phalloidin, hence suggesting that it is not a consequence of a nonspecific effect induced by cytochalasin D. The depolymerization of cytosolic F-actin occurred concomitantly with the beginning of the release of cytochrome *c* in the cytosol. Procaspase 3-like activation was observed later. Treatment of the cells with staurosporine led to a similar conclusion. Indeed, staurosporine induced the rapid destruction of cytosolic F-actin, except for some junctional actin still visible around the cell, concomitantly with the beginning of cytochrome *c* release from mitochondria. A delay of at least 60 min was then required to observe caspase 3-like activation. These observations suggest that the onset of staurosporine-induced cytochrome *c* release and procaspase activation is preceded by cytoskeletal disruption. Prevention of F-actin damage by phalloidin also interfered with F-actin disruption induced by staurosporine. However, in this case, phalloidin pretreatment only decreased the cytochrome *c* release and procaspase 3-like activation by a factor of 20 to 30%. The disruption of F-actin by staurosporine may therefore represent one of the multiple stimuli generated by staurosporine that trigger cytochrome *c* release and procaspase activation. Of interest, another apoptotic inducer, cisplatin, also alters F-actin fibers, and this phenomenon has been demonstrated to be responsible for apoptotic nuclear fragmentation (33). In this model, prevention of cisplatin-induced F-actin damage by phalloidin suppressed nuclear fragmentation, but prevention of nuclear apoptosis by Bcl-2 overexpression did not reduce the upstream damage to F-actin. This confirms that F-actin damage can trigger an apoptotic pathway (Fig. 14)—a phenomenon that can be amplified by the caspase 3-activated cleavage of the Ste20-related kinase SLK that further promotes actin disassembly and apoptosis (64). The actin microfilament network appears, therefore, to be a crucial upstream target which, when altered (e.g., by cytochalasin D, cisplatin, or staurosporine treatment) generates an apoptotic signaling pathway that activates cytochrome *c* release and procaspase activation.

When Hsp27 expression was analyzed, we confirmed earlier observations (19) that this protein delays F-actin damages caused by cytochalasin D. We also show that Hsp27 expression down-regulated F-actin damage caused by staurosporine treatment. In both cases, the protective effect of Hsp27 was dependent on its level of expression. Thus, in L929 cells, an expression of at least 0.45 ng/μg was necessary to detect a protective effect. This result is in agreement with the observation of Guay et al., who reported that an expression of Hsp27 of more than 2 ng/μg is necessary to protect CHO cells against F-actin disruption by cytochalasin D (19). It is also interesting that in antisense modified HeLa cells, a reduced level of Hsp27 expression sensitized these cells to staurosporine. Antisense inhibition of Hsp27 production, which is known to affect growth rate and cytoskeletal organization (43), may render the cytoskeleton more sensitive to apoptotic drugs. This may facilitate the activation of an F-actin disassembly to mitochondrial apoptotic pathway. Hence, the Hsp27-dependent reduced cytochrome *c* release from mitochondria may be related, at least in cytochalasin D-treated cells and to a certain extent in staurosporine-treated cells, to the Hsp27 ability to protect against F-actin network destruction. In this respect, it is interesting that F-actin microfilament breakdown has been reported as a key event in retinal neuronal apoptosis induced by elevated anti-Hsp27 antibody titers (72).

How does staurosporine rapidly damage F-actin, and how does F-actin network destruction trigger an apoptotic signaling pathway to mitochondria? One hypothesis is that F-actin depolymerization reorganizes the subcellular distribution of members of the Bcl2 family and/or alters integrin signaling pathways (21, 25, 83), which leads to Bid intracellular redistribution. However, there are conditions under which F-actin depolymerization does not trigger apoptosis, as for example during the cell cycle.

Another important question concerns F-actin damage: is this the unique upstream target that is activated in stress-induced apoptosis? The answer is negative, since we show here that the effect of phalloidin on cytochrome *c* and procaspase 3-like activation is only partial in the case of staurosporine treatment of the cells. Moreover, we show that etoposide does not drastically alters F-actin structure (37). In spite of this fact, Hsp27 expression can still interfere with Bid intracellular redistribution and mitochondrial cytochrome *c* loss. This leads to the hypothesis that still-unknown Hsp27-sensitive targets are involved in the etoposide and staurosporine signaling pathways triggering cytochrome *c* release from mitochondria.

Recently, we and others have reported that Hsp27 can interfere with procaspase 9 and 3 activation without altering cytochrome *c* release from mitochondria (9, 14, 55). This observation of a downstream effect of Hsp27 does not contradict the results presented here since a similar phenomenon can be observed in L929 cells expressing low levels (0.1 to 0.15 ng/μg) of murine Hsp27. Indeed, in these cells, cytochrome *c* release is not altered in spite of an inhibitory effect of Hsp27 toward procaspase 3 activation. Moreover, in postmitochondrial cell-free systems, Hsp27 was also reported to have a negative effect on procaspase 3-like activation by exogenous cytochrome *c* and dATP (10, 14) —a phenomenon which correlates with the interaction of Hsp27 with cytochrome *c* probably once this apoptogenic protein is released from mitochondria (9). However, this mechanism of action of Hsp27 is far from being understood since, as we show here, only a very small fraction of total endogenous cytochrome *c* interacts with Hsp27. This suggests that most cytochrome *c* does not interact with this chaperone protein and/or that only a very minor and particular form of Hsp27 can interact with this polypeptide. This observation suggests a chaperone-substrate type of interaction instead of the formation of complexes with define stoichiometry.

Taken together, our results lead to the possibility that Hsp27 may act both upstream and downstream of cytochrome *c* release. The upstream effect of Hsp27 appears to occur at the level of different pathways, one being probably related to F-actin architecture. Compared to the upstream effects described here, the downstream activity necessitates a lower level of Hsp27 expression to be active but is less efficient than the upstream activity at counteracting cell death. It is probable that the upstream F-actin pathway may require dimeric and non-phosphorylated Hsp27, since this is the structural form of Hsp27 which modulates actin polymerization in vitro (4). In contrast, the downstream effect may be linked to the chaperone activity associated with the large oligomers of Hsp27.

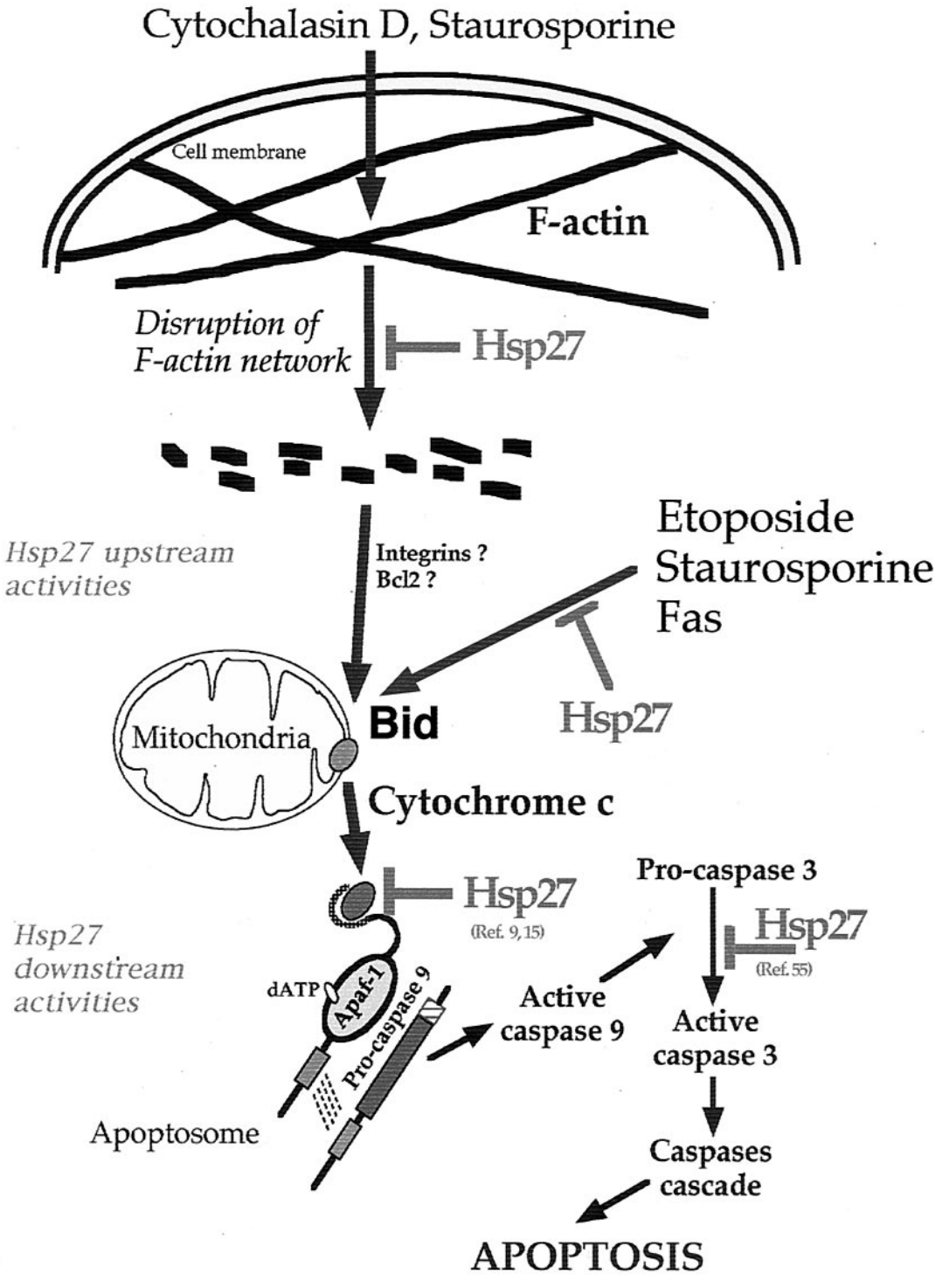

FIG. 14. Scheme of Hsp27-induced effects on apoptosis. Hsp27 reduces F-actin damage induced by apoptotic drugs (e.g., cytochalasin D and staurosporine) and thus attenuates the activation of the pathway that links F-actin damages to mitochondria. Activation of this pathway induces cytochrome *c* release, apoptosome formation, and procaspase activation. The mechanism of activation of this pathway is unknown but may be a consequence of altered integrin signaling pathway or changes in F-actin-dependent subcellular distribution of members of the Bcl-2 family such as Bid. Hsp27 also attenuates cytochrome *c* release in cells exposed to agents that do not rapidly destroy F-actin architecture (e.g., etoposide and Fas), suggesting that other upstream pathways are under the control of Hsp27 expression. Hsp27 also acts downstream of mitochondria by interfering with apoptosome formation, probably through its binding to cytochrome *c* once it is released from mitochondria. Hsp27 also appears to bind and negatively modulate caspase 3. In L929 cells, the upstream activity necessitates a higher level of Hsp27 expression (>0.45 ng/μg) compared to the downstream effect which is already detected in cells expressing Hsp27 (0.1 ng/μg).

These hypotheses are based on the facts that (i) Hsp27 large oligomers decrease in vitro caspase activation (10) and (ii) staurosporine as well as cytochalasin D induces a fraction of Hsp27 molecules to concentrate in a dimeric form (C. Paul, F. Manero, S. Virot, and A. P. Arrigo, unpublished data).

ACKNOWLEDGMENTS

F.M. and S.G. contributed equally to this work.

We thank Dominique Guillet for excellent technical assistance and Stéphane Ory and Frédéric Bard for their help with confocal microscopy.

C.P and F.M were supported by ATER and doctoral fellowships from the Ministère de l'Enseignement Supérieur et de la Recherche, respectively. This work was supported by the following grants: 5204 from the Association pour la Recherche sur le Cancer and the Région Rhône-Alpes (to A.-P.A.).

REFERENCES

1. **Arrigo, A.-P., and J. Landry.** 1994. Expression and function of the low-molecular-weight heat shock proteins, p. 335–373. *In* R. I. Morimoto, A. Tissieres, and C. Georgopoulos (ed.), The biology of heat shock proteins and molecular chaperones. Cold Spring Harbor Laboratory Press, Cold Spring Harbor, N.Y.
2. **Arrigo, A. P.** 1998. Small stress proteins: chaperones that act as regulators of intracellular redox state and programmed cell death. Biol. Chem. **379:**19–26.
3. **Beere, H. M., B. B. Wolf, K. Cain, D. D. Mosser, A. Mahboubi, T. Kuwana, P. Tailor, R. I. Morimoto, G. M. Cohen, and D. R. Green.** 2000. Heat-shock protein 70 inhibits apoptosis by preventing recruitment of procaspase-9 to the apaf-1 apoptosome. Nat. Cell Biol. **2:**469–475.
4. **Benndorf, R., K. Hayess, S. Ryazantsev, M. Wieske, J. Behlke, and G. Lutsch.** 1994. Phosphorylation and supramolecular organization of murine small heat shock protein HSP25 abolish its actin polymerization-inhibiting activity. J. Biol. Chem. **269:**20780–20784.
5. **Beresford, P. J., M. Jaju, R. S. Friedman, M. J. Yoon, and J. Lieberman.** 1998. A role for heat shock protein 27 in CTL-mediated cell death. J. Immunol. **161:**161–167.
6. **Boise, L. H., M. Gonzalez-Garcia, C. E. Postema, L. Ding, T. Lindsten, L. A. Turka, X. Mao, G. Nunez, and C. B. Thompson.** 1993. bcl-x, a bcl-2-related gene that functions as a dominant regulator of apoptotic cell death. Cell. **74:**597–608.
7. **Bossy-Wetzel, E., D. D. Newmeyer, and D. R. Green.** 1998. Mitochondrial cytochrome c release in apoptosis occurs upstream of DEVD-specific caspase activation and independently of mitochondrial transmembrane depolarization. EMBO J. **17:**37–49.
8. **Brown, S. B., K. Bailey, and J. Savill.** 1997. Actin is cleaved during constitutive apoptosis. Biochem. J. **323:**233–237.
9. **Bruey, J. M., C. Ducasse, P. Bonniaud, L. Ravagnan, S. A. Susin, C. Diaz-Latoud, S. Gurbuxani, A. P. Arrigo, G. Kroemer, E. Solary, and C. Garrido.** 2000. Hsp27 negatively regulates cell death by interacting with cytochrome c. Nat. Cell Biol. **2:**645–652.
10. **Bruey, J. M., C. Paul, A. Fromentin, S. Hilpert, A. P. Arrigo, E. Solary, and C. Garrido.** 2000. Differential regulation of HSP27 oligomerization in tumor cells grown in vitro and in vivo. Oncogene **19:**4855–4863.
11. **Desagher, S., A. Osen-Sand, A. Nichols, R. Eskes, S. Montessuit, S. Lauper, K. Maundrell, B. Antonsson, and J. C. Martinou.** 1999. Bid-induced conformational change of Bax is responsible for mitochondrial cytochrome c release during apoptosis. J. Cell Biol. **144:**891–901.
12. **Deveraux, Q. L., N. Roy, H. R. Stennicke, T. Van Arsdale, Q. Zhou, S. M. Srinivasula, E. S. Alnemri, G. S. Salvesen, and J. C. Reed.** 1998. IAPs block apoptotic events induced by caspase-8 and cytochrome c by direct inhibition of distinct caspases. EMBO J. **17:**2215–2223.
13. **Du, C., M. Fang, Y. Li, L. Li, and X. Wang.** 2000. Smac, a mitochondrial protein that promotes cytochrome c-dependent caspase activation by eliminating IAP inhibition. Cell **102:**33–42.
14. **Garrido, C., J. M. Bruey, A. Fromentin, A. Hammann, A. P. Arrigo, and E. Solary.** 1999. HSP27 inhibits cytochrome c-dependent activation of procaspase-9. FASEB J. **13:**2061–2070.
15. **Garrido, C., A. Fromentin, B. Bonnotte, N. Favre, M. Moutet, A. P. Arrigo, P. Mehlen, and E. Solary.** 1998. Heat shock protein 27 enhances the tumorigenicity of immunogenic rat colon carcinoma cell clones. Cancer Res. **58:**5495–5499.
16. **Garrido, C., P. Ottavi, A. Fromentin, A. Hammann, A. P. Arrigo, B. Chauffert, and P. Mehlen.** 1997. HSP27 as a mediator of confluence-dependent resistance to cell death induced by anticancer drugs. Cancer Res. **57:**2661–2667.
17. **Goldstein, J. C., N. J. Waterhouse, P. Juin, G. I. Evan, and D. R. Green.** 2000. The coordinate release of cytochrome c during apoptosis is rapid, complete and kinetically invariant. Nat. Cell Biol. **2:**156–162.
18. **Green, D. R., and J. C. Reed.** 1998. Mitochondria and apoptosis. Science **281:**1309–1312.
19. **Guay, J., H. Lambert, G. GingrasBreton, J. N. Lavoie, J. Huot, and J. Landry.** 1997. Regulation of actin filament dynamics by p38 map kinase-mediated phosphorylation of heat shock protein 27. J. Cell Sci. **110:**357–368.
20. **Guenal, I., C. Sidoti-de Fraisse, S. Gaumer, and B. Mignotte.** 1997. Bcl-2 and Hsp27 act at different levels to suppress programmed cell death. Oncogene **15:**347–360.
21. **Haldar, S., A. Basu, and C. M. Croce.** 1997. Bcl2 is the guardian of microtubule integrity. Cancer Res. **57:**229–233.
22. **Han, Z., K. Bhalla, P. Pantazis, E. A. Hendrickson, and J. H. Wyche.** 1999. Cif (cytochrome *c* efflux-inducing factor) activity is regulated by Bcl-2 and caspases and correlates with the activation of Bid. Mol. Cell. Biol. **19:**1381–1389.
23. **Hansen, R. K., I. Parra, P. Lemieux, S. Oesterreich, S. G. Hilsenbeck, and S. A. Fuqua.** 1999. Hsp27 overexpression inhibits doxorubicin-induced apoptosis in human breast cancer cells. Breast Cancer Res. Treat. **56:**187–196.
24. **Hockenbery, D., G. Nunez, C. Milliman, R. D. Schreiber, and S. J. Korsmeyer.** 1990. Bcl-2 is an inner mitochondrial membrane protein that blocks programmed cell death. Nature **348:**334–336.
25. **Hsu, Y. T., K. G. Wolter, and R. J. Youle.** 1997. Cytosol-to-membrane redistribution of Bax and Bcl-X(L) during apoptosis. Proc. Natl. Acad. Sci. USA **94:**3668–3672.
26. **Huot, J., F. Houle, S. Rousseau, R. G. Deschesnes, G. M. Shah, and J. Landry.** 1998. SAPK2/p38-dependent F-actin reorganization regulates early membrane blebbing during stress-induced apoptosis. J. Cell Biol. **143:**1361–1373.
27. **Huot, J., F. Houle, D. R. Spitz, and J. Landry.** 1996. HSP27 phosphorylation-mediated resistance against actin fragmentation and cell death induced by oxidative stress. Cancer Res. **56:**273–279.
28. **Jäättelä, M.** 1995. Over-expression of Hsp70 confers tumorigenicity to mouse fibrosarcoma cells. Int. J. Cancer **60:**689–693.
29. **Jäättelä, M., D. Wissing, K. Kokholm, T. Kallunki, and M. Egeblad.** 1998. Hsp70 exerts its anti-apoptotic function downstream of caspase-3-like proteases. EMBO J. **17:**6124–6134.
30. **Jakob, U., M. Gaestel, K. Engels, and J. Buchner.** 1993. Small heat shock proteins are molecular chaperones J. Biol. Chem. **268:**1517–1520.
31. **Kluck, R. M., E. Bossy-Wetzel, D. R. Green, and D. D. Newmeyer.** 1997. The release of cytochrome c from mitochondria: a primary site for Bcl-2 regulation of apoptosis. Science **275:**1132–1136.
32. **Kohler, C., A. Gahm, T. Noma, A. Nakazawa, S. Orrenius, and B. Zhivotovsky.** 1999. Release of adenylate kinase 2 from the mitochondrial intermembrane space during apoptosis. FEBS Lett. **447:**10–12.
33. **Kruidering, M., B. van de Water, Y. Zhan, J. J. Baelde, E. Heer, G. J. Mulder, J. L. Stevens, and J. F. Nagelkerke.** 1998. Cisplatin effects on F-actin and matrix proteins precede renal tubular cell detachment and apoptosis in vitro. Cell Death Differ. **5:**601–614.
34. **Lavoie, J. N., G. Gingras-Breton, R. M. Tanguay, and J. Landry.** 1993. Induction of chinese hamster HSP27 gene expression in mouse cells confers resistance to heat shock J. Biol. Chem. **268:**3420–3429.
35. **Lavoie, J. N., E. Hickey, L. A. Weber, and J. Landry.** 1993. Modulation of actin microfilament dynamics and fluid phase pinocytosis by phosphorylation of heat shock protein 27. J. Biol. Chem. **268:**24210–24214.
36. **Lavoie, J. N., H. Lambert, E. Hickey, L. A. Weber, and J. Landry.** 1995. Modulation of cellular thermoresistance and actin filament stability accompanies phosphorylation-induced changes in the oligomeric structure of heat shock protein 27. Mol. Cell. Biol. **15:**505–516.
37. **Levee, M. G., M. I. Dabrowska, J. L. Lelli, Jr., and D. B. Hinshaw.** 1996. Actin polymerization and depolymerization during apoptosis in HL-60 cells. Am. J. Physiol. **271:**C1981–C1992.
38. **Li, C.-Y., J.-S. Lee, Y.-G. Ko, J.-I. Kim, and J.-S. Seo.** 2000. Heat shock protein 70 inhibits downstream of cytochrome *c* release and upstream of caspase-3 activation. J. Biol. Chem. **275:**25665–25671.
39. **Li, H., H. Zhu, C. J. Xu, and J. Yuan.** 1998. Cleavage of BID by caspase 8 mediates the mitochondrial damage in the Fas pathway of apoptosis. Cell **94:**491–501.
40. **Li, P., D. Nijhawan, I. Budihardjo, S. M. Srinivasula, M. Ahmad, E. S. Alnemri, and X. Wang.** 1997. Cytochrome c and dATP-dependent formation of Apaf-1/caspase-9 complex initiates an apoptotic protease cascade. Cell **91:**479–489.
41. **Low, I., P. Dancker, and T. Wieland.** 1975. Stabilization of F-actin by phalloidin. Reversal of the destabilizing effect of cytochalasin B. FEBS Lett. **54:**263–265.
42. **Luo, X., I. Budihardjo, H. Zou, C. Slaughter, and X. Wang.** 1998. Bid, a Bcl2 interacting protein, mediates cytochrome c release from mitochondria in response to activation of cell surface death receptors. Cell **94:**481–490.
43. **Mairesse, N., S. Horman, R. Mosselmans, and P. Galand.** 1996. Antisense inhibition of the 27 kDa heat shock protein production affects growth rate and cytoskeletal organization in MCF-7 cells. Cell. Biol. Int. **20:**205–212.
44. **Martinou, I., S. Desagher, R. Eskes, B. Antonsson, E. Andre, S. Fakan, and J. C. Martinou.** 1999. The release of cytochrome c from mitochondria during

apoptosis of NGF-deprived sympathetic neurons is a reversible event. J. Cell Biol. **144:**883–889.
45. **Mehlen, P., V. Coronas, V. Ljubic-Thibal, C. Ducasse, L. Granger, F. Jourdan, and A. P. Arrigo.** 1999. Small stress protein Hsp27 accumulation during dopamine-mediated differentiation of rat olfactory neurons counteracts apoptosis. Cell Death Differ. **6:**227–233.
46. **Mehlen, P., E. Hickey, L. Weber, and A.-P. Arrigo.** 1997. Large unphosphorylated aggregates as the active form of hsp27 which controls intracellular reactive oxygen species and glutathione levels and generates a protection against TNFα in NIH-3T3-ras cells. Biochem. Biophys. Res. Comm. **241:** 187–192.
47. **Mehlen, P., A. Mehlen, J. Godet, and A.-P. Arrigo.** 1997. hsp27 as a switch between differentiation and apoptosis in murine embryonic stem cells. J. Biol. Chem. **272:**31657–31665.
48. **Mehlen, P., X. Préville, P. Chareyron, J. Briolay, R. Klemenz, and A.-P. Arrigo.** 1995. Constitutive expression of human hsp27, Drosophila hsp27, or human alpha B-crystallin confers resistance to TNF- and oxidative stress-induced cytotoxicity in stably transfected murine L929 fibroblasts. J. Immunol. **154:**363–374.
49. **Mehlen, P., X. Préville, C. Kretz-Remy, and A.-P. Arrigo.** 1996. Human hsp27, Drosophila hsp27 and human αB-crystallin expression-mediated increase in glutathione is essential for the protective activity of these protein against TNFα-induced cell death. EMBO J. **15:**2695–2706.
50. **Mehlen, P., K. Schulze-Osthoff, and A.-P. Arrigo.** 1996. Small stress proteins as novel regulators of apoptosis: heat shock protein 27 blocks Fas/APO-1- and staurosporine-induced cell death. J. Biol. Chem. **271:**16510–16514.
51. **Merry, D. E., and S. J. Korsmeyer.** 1997. Bcl-2 gene family in the nervous system. Annu. Rev. Neurosci. **20:**245–267.
52. **Miron, T., K. Vancompernolle, J. Vandekerckhove, M. Wilchek, and B. Geiger.** 1991. A 25-kD inhibitor of actin polymerization is a low molecular mass heat shock protein. J. Cell Biol. **114:**255–261.
53. **Mosser, D. D., A. W. Caron, L. Bourget, C. Denis-Larose, and B. Massie.** 1997. Role of the human heat shock protein hsp70 in protection against stress-induced apoptosis. Mol. Cell. Biol. **17:**5317–5327.
54. **Nicholson, D. W., and N. A. Thornberry.** 1997. Caspases: killer proteases. Trends Biochem. Sci. **22:**299–306.
55. **Pandey, P., R. Farber, A. Nakazawa, S. Kumar, A. Bharti, C. Nalin, R. Weichselbaum, D. Kufe, and S. Kharbanda.** 2000. Hsp27 functions as a negative regulator of cytochrome c-dependent activation of procaspase-3. Oncogene **19:**1975–1981.
56. **Pandey, P., A. Saleh, A. Nakazawa, S. Kumar, S. M. Srinivasula, V. Kumar, R. Weichselbaum, C. Nalin, E. S. Alnemri, D. Kufe, and S. Kharbanda.** 2000. Negative regulation of cytochrome c-mediated oligomerization of Apaf-1 and activation of procaspase-9 by heat shock protein 90. EMBO J. **19:**4310–4322.
57. **Paul, C., and A. P. Arrigo.** 2000. Comparison of the protective activities generated by two survival proteins: Bcl-2 and Hsp27 in L929 murine fibroblasts exposed to menadione or staurosporine. Exp. Gerontol. **35:**757–766.
58. **Préville, X., M. Gaestel, and A. P. Arrigo.** 1998. Phosphorylation is not essential for protection of L929 cells by Hsp25 against H2O2-mediated disruption actin cytoskeleton, a protection which appears related to the redox change mediated by Hsp25. Cell Stress Chaperones **3:**177–187.
59. **Preville, X., F. Salvemini, S. Giraud, S. Chaufour, C. Paul, G. Stepien, M. V. Ursini, and A. P. Arrigo.** 1999. Mammalian small stress proteins protect against oxidative stress through their ability to increase glucose-6-phosphate dehydrogenase activity and by maintaining optimal cellular detoxifying machinery. Exp. Cell Res. **247:**61–78.
60. **Préville, X., H. Schultz, U. Knauf, M. Gaestel, and A. P. Arrigo.** 1998. Analysis of the role of Hsp25 phosphorylation reveals the importance of the oligomerization state of this small heat shock protein in its protective function against TNFalpha- and hydrogen peroxide-induced cell death. J. Cell. Biochem. **69:**436–452.
61. **Reed, J. C.** 1997. Cytochrome c: can't live with it–can't live without it. Cell **91:**559–562.
62. **Rogalla, T., M. Ehrnsperger, X. Preville, A. Kotlyarov, G. Lutsch, C. Ducasse, C. Paul, M. Wieske, A. P. Arrigo, J. Buchner, and M. Gaestel.** 1999. Regulation of Hsp27 oligomerization, chaperone function, and protective activity against oxidative stress/tumor necrosis factor alpha by phosphorylation J. Biol. Chem. **274:**18947–18956.
63. **Rosse, T., R. Olivier, L. Monney, M. Rager, S. Conus, I. Fellay, B. Jansen, and C. Borner.** 1998. Bcl-2 prolongs cell survival after Bax-induced release of cytochrome c. Nature **391:**496–499.
64. **Sabourin, L. A., K. Tamai, P. Seale, J. Wagner, and M. A. Rudnicki.** 2000. Caspase 3 cleavage of the Ste20-related kinase SLK releases and activates an apoptosis-inducing kinase domain and an actin-disassembling region. Mol. Cell. Biol. **20:**684–696.
65. **Samali, A., J. Cai, B. Zhivotovsky, D. P. Jones, and S. Orrenius.** 1999. Presence of a pre-apoptotic complex of pro-caspase-3, Hsp60 and Hsp10 in the mitochondrial fraction of Jurkat cells. EMBO J. **18:**2040–2048.
66. **Samali, A., and T. G. Cotter.** 1996. Heat shock proteins increase resistance to apoptosis. Exp. Cell Res. **223:**163–170.
67. **Samali, A., J. Robertson, E. Peterson, F. Manero, L. van Zeijl, C. Paul, I. A. Cotgreave, A.-P. Arrigo, and S. Orrenius.** 2001. Small heat shock proteins protect mitochondria of thermotolerant cells. Cell Stress Chaperones **6:**49–58.
68. **Shimizu, S., M. Narita, and Y. Tsujimoto.** 1999. Bcl-2 family proteins regulate the release of apoptogenic cytochrome c by the mitochondrial channel VDAC. Nature **399:**483–487.
69. **Susin, S. A., H. K. Lorenzo, N. Zamzami, I. Marzo, C. Brenner, N. Larochette, M. C. Prevost, P. M. Alzari, and G. Kroemer.** 1999. Mitochondrial release of caspase-2 and -9 during the apoptotic process. J. Exp. Med. **189:**381–394.
70. **Susin, S. A., H. K. Lorenzo, N. Zamzami, I. Marzo, B. E. Snow, G. M. Brothers, J. Mangion, E. Jacotot, P. Costantini, M. Loeffler, N. Larochette, D. R. Goodlett, R. Aebersold, D. P. Siderovski, J. M. Penninger, and G. Kroemer.** 1999. Molecular characterization of mitochondrial apoptosis-inducing factor. Nature **397:**441–446.
71. **Takayama, S., D. N. Bimston, S. Matsuzawa, B. C. Freeman, C. Aime-Sempe, Z. Xie, R. I. Morimoto, and J. C. Reed.** 1997. BAG-1 modulates the chaperone activity of Hsp70/Hsc70. EMBO J. **16:**4887–4896.
72. **Tezel, G., and M. B. Wax.** 2000. The mechanisms of hsp27 antibody-mediated apoptosis in retinal neuronal cells. J. Neurosci. **20:**3552–3562.
73. **Thornberry, N. A., and Y. Lazebnik.** 1998. Caspases: enemies within. Science **281:**1312–1316.
74. **Trounce, I., Y. Kim, A. Jun, and D. Wallace.** 1996. Assessment of mitochondrial oxidative phosphorylation in patient muscle biopsies, lymphoblasts, and transmitochondrial cell lines. Methods Enzymol. **264:**484–509.
75. **Van de Water, B., M. Kruidering, and J. F. Nagelkerke.** 1996. F-actin disorganization in apoptotic cell death of cultured rat renal proximal tubular cells. Am. J. Physiol. **270:**F593–F603.
76. **Vaux, D. L., S. Cory, and J. M. Adams.** 1988. Bcl-2 gene promotes haemopoietic cell survival and cooperates with c-myc to immortalize pre-B cells. Nature **335:**440–442.
77. **Verhagen, A. M., P. G. Ekert, M. Pakusch, J. Silke, L. M. Connolly, G. E. Reid, R. L. Moritz, R. J. Simpson, and D. L. Vaux.** 2000. Identification of DIABLO, a mammalian protein that promotes apoptosis by binding to and antagonizing IAP proteins. Cell **102:**43–53.
78. **Wagstaff, M. J., Y. Collaco-Moraes, J. Smith, J. S. de Belleroche, R. S. Coffin, and D. S. Latchman.** 1999. Protection of neuronal cells from apoptosis by Hsp27 delivered with a herpes simplex virus-based vector. J. Biol. Chem. **274:**5061–5069.
79. **Wolter, K. G., Y. T. Hsu, C. L. Smith, A. Nechushtan, X. G. Xi, and R. J. Youle.** 1997. Movement of Bax from the cytosol to mitochondria during apoptosis. J. Cell Biol. **139:**1281–1292.
80. **Xanthoudakis, S., S. Roy, D. Rasper, T. Hennessey, Y. Aubin, R. Cassady, P. Tawa, R. Ruel, A. Rosen, and D. W. Nicholson.** 1999. Hsp60 accelerates the maturation of pro-caspase-3 by upstream activator proteases during apoptosis EMBO J. **18:**2049–2056.
81. **Yahara, I., F. Harada, S. Sekita, K. Yoshihira, and S. Natori.** 1982. Correlation between effects of 24 different cytochalasins on cellular structures and cellular events and those on actin in vitro. J. Cell Biol. **92:**69–78.
82. **Yang, J., X. Liu, K. Bhalla, C. N. Kim, A. M. Ibrado, J. Cai, T. I. Peng, D. P. Jones, and X. Wang.** 1997. Prevention of apoptosis by Bcl-2: release of cytochrome c from mitochondria blocked. Science **275:**1129–1132.
83. **Zhang, Z., K. Vuori, J. C. Reed, and E. Ruoslahti.** 1995. The alpha 5 beta 1 integrin supports survival of cells on fibronectin and up-regulates Bcl-2 expression. Proc. Natl. Acad. Sci. USA **92:**6161–6165.
84. **Zhuang, J., D. Dinsdale, and G. M. Cohen.** 1998. Apoptosis, in human monocytic THP.1 cells, results in the release of cytochrome c from mitochondria prior to their condensation, formation of outer membrane discontinuities and reduction in inner membrane potential. Cell Death Differ. **5:**953–962.